Improving the neutrino mass hierarchy identification with inelasticity measurement in PINGU and ORCA

Mathieu Ribordy[1,*] and A. Yu. Smirnov[2,†]

[1]*High Energy Physics Laboratory, École Polytechnique Fédérale, CH-1015 Lausanne, Switzerland*
[2]*The Abdus Salam International Centre for Theoretical Physics, I-34100 Trieste, Italy*

Multimegaton scale in under-ice and underwater detectors of atmospheric neutrinos with a few GeV energy threshold (PINGU, ORCA) open up new possibilities in the determination of neutrino properties, and in particular the neutrino mass hierarchy. With a dense array of optical modules it will be possible to determine the inelasticity, y, of the charged current ν_μ events in addition to the neutrino energy E_ν and the muon zenith angle θ_μ. The discovery potential of the detectors will substantially increase with the measurement of y. It will enable (i) a partial separation of the neutrino and antineutrino signals, (ii) a better reconstruction of the neutrino direction, (iii) the reduction of the neutrino parameters degeneracy, (iv) a better control of systematic uncertainties, and (v) a better identification of the ν_μ events. It will improve the sensitivity to the CP-violation phase. The three-dimensional (E_ν, θ_μ, y), ν_μ oscillograms with the kinematical as well as the experimental smearing are computed. We present the asymmetry distributions in the $E_\nu - \theta_\mu$ plane for different intervals of y and study their properties. We show that the inelasticity information reduces the effect of degeneracy of parameters by 30%. With the inelasticity, the total significance of establishing mass hierarchy may increase by (20–50)%, thus effectively increasing the volume of the detector by a factor of 1.5–2.

PACS numbers: 14.60.Pq

I. INTRODUCTION

Multimegaton scale atmospheric neutrino detectors with a few GeV energy threshold have an enormous and largely unexplored physics potential. These detectors are sensitive to the oscillatory patterns due to the 1–3 mixing in the neutrino energy-zenith angle $(E_\nu - \theta_\nu)$ plane. The patterns have several salient features, which include the Mikheyev-Smirnov-Wolfenstein resonance peaks due to oscillations in the mantle $(E_\nu \sim 6 \text{ GeV})$ and the core $(E_\nu \sim 4 \text{ GeV})$ as well as the parametric enhancement ridges at $E_\nu \sim (4\text{–}12) \text{ GeV}$ which are realized for the core crossing neutrino trajectories (see [1] for a detailed description and [2] for a recent review and references). The patterns differ for neutrinos and antineutrinos and strongly depend on the type of neutrino mass hierarchy. In particular, the indicated features appear in the neutrino channels in the case of normal mass hierarchy (NH) and in the antineutrino channels in the case of inverted hierarchy (IH) (in the two neutrino approximation, inversion of the mass hierarchy is equivalent to switching the neutrino and antineutrino oscillation patterns). This opens up a possibility to establish the neutrino mass hierarchy and also to measure the deviation of the 2–3 mixing from maximal as well as the 1–3 mass splitting. Once the hierarchy is established, one can consider a possibility to measure the CP-violation phase.

Multimegaton detectors are expected to record of the order of 10^5 events a year. Such a large statistics allows,

in principle, to compensate for shortcomings related to flavor identification of events and reconstruction of their energy and angular characteristics. With so high statistics, one can select some particular events in certain kinematical regions, which are most sensitive to a given neutrino parameter, thus reducing the effect of degeneracy of parameters, etc.

PINGU (Precision IceCube Next-Generation Upgrade) [3], the IceCube DeepCore [4] augmented with a denser instrumentation in its center, and ORCA (Oscillation Research with Cosmics in the Abyss) [5] projects are possible future realizations of these multimegaton scale detectors.

A simplified estimation of the sensitivity to the mass hierarchy of the DeepCore (DC) experiment has been performed in [6]. Due to the high energy threshold (>10 GeV), DC has a low sensitivity to the resonance pattern and therefore to the hierarchy. The sensitivity of DC to deviation of the 2–3 mixing from maximal has been explored in [7].

The idea to send a neutrino beam from Fermilab to PINGU to determine the mass hierarchy has been elaborated in [8].

A possibility to use PINGU and the atmospheric neutrino flux for the identification of the neutrino mass hierarchy (MH) and search for the CP-violation effects was recently explored in [9]. The strategy is based on the measurement of the $E_\nu - \theta_\nu$ distribution of the sum of muon neutrino and antineutrino events. The smearing of the distribution over θ_ν and E_ν has been performed that takes into account the accuracy of reconstruction of the neutrino energy and direction.

*mathieu.ribordy@epfl.ch
†smirnov@ictp.it

The estimator of discovery potential S (the hierarchy asymmetry) has been introduced [9], which allows one to make quick evaluation of sensitivities of the detector to neutrino mass hierarchy as well as to other parameters. For the ij bin in the reconstructed neutrino energy (i) and zenith angle (j), the asymmetry is defined as

$$S_{\nu,ij} = \frac{N_{\nu,ij}^{\mathrm{IH}} - N_{\nu,ij}^{\mathrm{NH}}}{\sqrt{N_{\nu,ij}^{\mathrm{NH}}}}.$$

Here $N_{\nu,ij}^{\mathrm{NH}}$ and $N_{\nu,ij}^{\mathrm{IH}}$ are the numbers of events in the ij bin for the normal and the inverted mass hierarchies correspondingly. The moduli of the asymmetry $|S_{\nu,ij}|$ gives the statistical significance for the identification of the mass hierarchy. The asymmetry allows one to explore in a transparent way the dependence of sensitivities on the experimental energy and angular resolutions, on degeneracies of parameters and on various systematic errors. In [9] it was shown that the hierarchy can be established at $(3\text{--}10)\sigma$ level after five years of operation of PINGU depending on the energy and angular resolutions and on the size of the systematic error.

A final answer concerning the sensitivity should follow from the detailed Monte Carlo simulation of the distributions of events. That should take into account realistic parameters of the detectors after their geometries are determined. Then, in a simple approach, the sensitivity can be obtained from the fit of the simulated distributions with the distributions computed for the cases of normal and inverted mass hierarchies. The fit can be done using Poisson statistics without binning. Results of a "toy" Monte Carlo study for large volume detectors have been presented in [10]. The physics potential of PINGU and ORCA was further explored in [10,11].

As it was discussed in [9], several factors dilute the significance of the MH identification, although at the probability level the effect of inversion of the hierarchy is of the order 1. Indeed,

(i) the hierarchy asymmetry has opposite signs in different kinematical regions. Therefore smearing over the angle and energy $E_\nu - \theta_\nu$ leads to a substantial decrease of the observable effect. The smearing originates from finite energy and angular resolutions of the detector (experimental smearing) and due to difference of the neutrino and muon directions (kinematical smearing).

(ii) The hierarchy asymmetry has different signs for neutrinos and antineutrinos. Therefore summing up the neutrino and antineutrino signals leads to a partial cancellation of the effect.

(iii) The presence of both ν_μ and ν_e flavors in the original atmospheric neutrino flux leads, in general, to a suppression of oscillation effects. The suppression becomes weaker at high energies, where the ν_e flux is small.

(iv) Current uncertainties of the oscillation parameters, such as Δm_{32}^2 and θ_{23}^2, further reduce identification power, since the effect of inversion of the mass hierarchy can be partly mimicked by changes of these parameters.

(v) The sample of ν_μ events is contaminated by contributions from ν_τ and ν_e charged current (CC) interactions and neutral current (NC) interactions of all neutrino species. In particular, ν_τ's generated via oscillations produce tau leptons, which decay into muons in 18% of the cases, thus appearing as ν_μ events. Also ν_e and NC interactions can mimic ν_μ events due to muon-pion misidentification. These events produce an additional effective smearing of the oscillatory pattern.

All this renders the quest of the neutrino mass hierarchy difficult. Some (probably modest) developments of technology are required. This includes the selection of certain geometry of the detector, the upgrade of the optical modules, further developments of the time analysis of events, etc. On the other hand, some particular ways to analyze the information obtained can also improve the sensitivity.

In this connection, we explore improvements of the sensitivity to the neutrino MH due to the measurement of the inelasticity, $y \approx 1 - E_\mu/E_\nu$, of the charged current ν_μ events. As we will show, this new ingredient in the analysis enables us to alleviate some of the problems mentioned above. In particular, it allows us to effectively separate the ν_μ and $\bar{\nu}_\mu$ signals, and thus to reduce the partial cancellation of their contributions to the MH asymmetry. The idea was mentioned in [12]. Using the inelasticity will also enable to reduce the kinematical smearing effect and degeneracy of parameters. It will lead to a better flavor identification of the ν_μ events.

The paper is organized as follows. In Sec. II, we describe the ν_μ events, their detection characteristics, relevant kinematics and cross sections. In Sec. III, possible improvements of the sensitivity to the mass hierarchy and other neutrino parameters due to the inelasticity measurements are discussed. In Sec. IV, we compute the three-dimensional distributions of events in the reconstructed neutrino energy, E_ν, the muon zenith angle, θ_μ, and y variables, which take into account the kinematical smearing. We explore the properties of these 3D distributions and find the corresponding hierarchy asymmetry plots. In Sec. V, we present results of smearing of the distributions over the finite experimental resolutions of observables: the muon and hadron cascade energies and the muon angle. We then compute the total significance of identification of the mass hierarchy and its dependence on the possible accuracy of the measurements of the energies and angles (experimental smearing). We estimate how the measurements of inelasticity reduce the effect of degeneracy of the mass hierarchy and mass splitting Δm_{32}^2. Section VI contains a discussion of the results and outlook.

II. ν_μ EVENTS AND INELASTICITY

A. ν_μ events

In this paper we concentrate on the ν_μ events induced by the charged current weak interactions:

$$\nu_\mu + N \rightarrow \mu + h, \tag{1}$$

where h refers to the hadron system in the final state. Observables associated to the reaction (1) are the energy of the muon E_μ, its direction characterized by the zenith and azimuth angles θ_μ and ϕ_μ, and the cascade energy (the total energy in hadrons), E_h.

At the energies we consider, from a few GeV up to ≈ 30 GeV, the cascade direction is not meaningful on an event basis. Indeed, the cascade energy is shared in a variable mixture between light mesons and heavier hadrons, which leads to a highly random and anisotropic Cherenkov photons emission. Contrary to muons, the energy release from cascades is approximately "pointlike," given the sparsely instrumented detector arrays under investigation.

The reconstruction of the ν_μ event consisting of recorded photons (hits) from the combined emission from a vertex shower and a muon track in this case, can be performed well at low energy using prescriptions in [13]. The visible cascade energy, the muon track length (i.e., its energy), and incoming muon direction can be extracted. Moreover, the impact of the short scattering length of Cherenkov photons for a dense detector in ice is expected to be rather mild as it will be argued later. As most hits are undelayed, a good reconstruction accuracy of the muon incoming direction as well as a clear separation of the shower and muon signatures are expected.

Thus, the set of observables $\{E_\mu, \theta_\mu, \phi_\mu, E_h\}$ constitutes a rather exhaustive description of the CC ν_μ interaction. The original neutrino energy is determined through

$$E_\nu = E_h + E_\mu - m_N, \tag{2}$$

where m_N is the nucleon mass.

B. Inelasticity and kinematics of the process

The inelasticity y is defined as

$$y \equiv \frac{E_\nu - E_\mu}{E_\nu}. \tag{3}$$

Let us consider the angle between the neutrino and the produced muon, β. The square of the transfer momentum q^2 equals

$$q^2 \equiv (p_\nu - p_\mu)^2 = -2E_\nu(E_\mu - |\mathbf{p}_\mu| \cos \beta) + m_\mu^2,$$

so that $Q^2 \equiv -q^2$ equals

$$Q^2 = 2E_\nu E_\mu \left(1 - \frac{|\mathbf{p}_\mu|}{E_\mu} \cos \beta\right) - m_\mu^2.$$

This gives

$$\cos \beta = \frac{E_\mu}{|\mathbf{p}_\mu|}\left(1 - \frac{Q^2 + m_\mu^2}{2E_\nu E_\mu}\right). \tag{4}$$

In terms of the Bjorken variable

$$x \equiv \frac{Q^2}{2(p_N q)} = \frac{Q^2}{2m_N(E_\nu - E_\mu)}$$

we have

$$Q^2 = 2xy m_N E_\nu,$$

where we used (3). Insertion of this expression into (4) gives

$$\cos \beta = \frac{E_\mu}{|\mathbf{p}_\mu|}\left[1 - \frac{2xy m_N E_\nu + m_\mu^2}{2E_\nu E_\mu}\right]. \tag{5}$$

Notice that with a decrease of $\mathbf{p}_\mu$, $\cos \beta \rightarrow \pm 1$ when $x \rightarrow 0, 1$. We can rewrite (5) as

$$\cos \beta = 1 - 2xy \zeta(E_\nu, x, y),$$

where

$$\zeta(E_\nu, x, y) = \frac{m_\mu^2 + 2m_N E_\nu xy - 2E_\nu(E_\mu - |\mathbf{p}_\mu|)}{4E_\nu xy|\mathbf{p}_\mu|}.$$

Here $E_\mu = E_\mu(E_\nu, y)$ and $\mathbf{p}_\mu = \mathbf{p}_\mu(E_\nu, y)$. If $\mathbf{p}_\mu \approx E_\mu \gg m_\mu$, we obtain neglecting m_μ

$$\zeta(E_\nu, y) \approx \frac{m_N}{2E_\mu}.$$

Let us find the limits in which $c_\beta \equiv \cos \beta$ changes. Varying x, we obtain for $x = 0$ that $c_\beta \approx E_\mu/|\mathbf{p}_\mu| > 1$, so that $c_\beta^{\max} = 1$. For not very small $|\mathbf{p}_\mu|$ (and we will consider $|\mathbf{p}_\mu| > m_N$) the minimal value of c_β corresponds to $x = 1$:

$$c_\beta^{\min} = \frac{E_\mu}{|\mathbf{p}_\mu|}\left[1 - \frac{2m_N(E_\nu - E_\mu) + m_\mu^2}{2E_\nu E_\mu}\right]$$

$$\approx \frac{E_\mu}{|\mathbf{p}_\mu|}\left[1 - \frac{2m_N}{E_\mu}\left(1 - \frac{E_\mu}{E_\nu}\right)\right], \tag{6}$$

or $\sin \beta^{\min}/2 \sim \sqrt{y m_N/E_\mu}$.

For a given muon direction, the neutrino direction is determined by the angle β and the azimuthal angle ϕ with respect to the plane formed by the muon momentum and axis x. It is straightforward (see Appendix A) to find the relation between the neutrino zenith angle θ_ν and the muon zenith angle θ_μ:

$$c_\nu = c_\beta c_\mu + s_\beta s_\mu c_\phi, \tag{7}$$

where $c_\nu \equiv \cos \theta_\nu$, $c_\mu \equiv \cos \theta_\mu$, and $c_\phi \equiv \cos \phi$.

According to (7) for fixed β the maximal and minimal values of c_ν correspond to $c_\phi = \pm 1$ and equal

$$c_\nu^{\max} = \cos(\theta_\mu - \beta), \qquad c_\nu^{\min} = \cos(\theta_\mu + \beta). \quad (8)$$

C. Cross sections

In our calculations of Secs. IV and V we will use the deep inelastic scattering (DIS) cross section only. We neglect the contributions of the single pion production and quasielastic scattering processes. This will lead to conservative estimations of sensitivities, as the reduced momentum transfer translates into a smaller angle between the muon and the neutrino directions. In any case the relative importance of these processes becomes negligible above ≈ 5 GeV, and below ≈ 5 GeV, detector resolutions and effective volumes are strongly limited.

The differential CC cross sections of the ν and $\bar\nu$ DIS on an isonucleon $N = \frac{1}{2}(n + p)$ equal

$$\frac{d^2\sigma_\nu^{CC}}{dx dy}(E_\nu, x, y)$$
$$= \frac{G_F^2 m_N x E_\nu}{\pi}[(q + s - c) + (1 - y)^2(\bar q - \bar s + \bar c)], \quad (9)$$

$$\frac{d^2\sigma_{\bar\nu}^{CC}}{dx dy}(E_\nu, x, y)$$
$$= \frac{G_F^2 m_N x E_\nu}{\pi}[(\bar q - \bar s + \bar c) + (1 - y)^2(q + s - c)], \quad (10)$$

where $q \equiv u + d + s + c$, $\bar q \equiv \bar u + \bar d + \bar s + \bar c$, and the quark densities $u = u(x, Q^2)$, etc., are described by the CTEQ5 parton distribution functions in the standard $\overline{MS}$ scheme [14], valid down to $Q^2 \approx 1$ GeV^2.

The limits of x integration of the cross sections are in the interval $\{x_{\min}, x_{\max}\} = \{x(c_\beta = 1), 1\}$, and y integration runs from 0 to $y_{\max} = 1 - m_\mu/E_\nu$.

Integrating the cross sections (9) and (10) over x we obtain

$$\frac{d\sigma_\nu^{CC}}{dy} = [-a_0 - a_1(1 - y)^2]10^{-38} \text{ cm}^2 \frac{E_\nu}{1 \text{ GeV}},$$
$$\frac{d\sigma_{\bar\nu}^{CC}}{dy} = [-b_0 - b_1(1 - y)^2)]10^{-38} \text{ cm}^2 \frac{E_\nu}{1 \text{ GeV}},$$

where $a_0 = 0.72$, $a_1 = 0.06$, $b_0 = 0.09$, and $b_1 = 0.69$. Then the normalized inelasticity distributions equal

$$p_\nu \equiv -\frac{1}{\sigma_\nu}\frac{d\sigma_\nu}{dy} \approx \frac{a_0 + a_1(y - 1)^2}{a_0 + a_1/3}, \quad (11)$$

$$p_{\bar\nu} \equiv -\frac{1}{\sigma_{\bar\nu}}\frac{d\sigma_{\bar\nu}}{dy} \approx \frac{b_0 + b_1(y - 1)^2}{b_0 + b_1/3}. \quad (12)$$

Here, we have dropped the very weak E_ν dependence in the range of interest and considered the limit $m_\mu \to 0$.

D. Number of events

The number of neutrino and antineutrino events in the case of NH, N_ν^{NH}, and $N_{\bar\nu}^{NH}$ in a given ij bin of the size $\Delta_i \cos\theta_\nu$, $\Delta_j E_\nu$ equals

$$N_\nu^{NH} = \int_{\Delta_i \cos\theta_\nu} d\cos\theta_\nu \int_{\Delta_j E_\nu} dE_\nu \rho_\nu^{NH}(E_\nu, \cos\theta_\nu),$$

and for $N_{\bar\nu}^{NH}$ one needs to substitute $\rho_\nu^{NH} \to \rho_{\bar\nu}^{NH}$. Here

$$\rho_\nu^{NH} \equiv 2\pi N_A n_{ice} V_{eff} T \sigma^{CC} \Phi_\mu^0 \left[P_{\mu\mu}^{NH} + \frac{1}{r}P_{e\mu}^{NH} \right], \quad (13)$$

$$\rho_{\bar\nu}^{NH} \equiv 2\pi N_A n_{ice} V_{eff} T \bar\sigma^{CC} \bar\Phi_\mu^0 \left[\bar P_{\mu\mu}^{NH} + \frac{1}{\bar r}\bar P_{e\mu}^{NH} \right]. \quad (14)$$

In (13) and (14),

$$r \equiv \frac{\Phi_\mu^0}{\Phi_e^0}, \qquad \bar r \equiv \frac{\bar\Phi_\mu^0}{\bar\Phi_e^0}$$

are the flavor ratios, where $\Phi_\alpha^0 = \Phi_\alpha^0(E_\nu, \theta_\nu)$ are the neutrino fluxes at production; $P_{\alpha\beta}^{NH}$ and $\bar P_{\alpha\beta}^{NH}$ are the $\nu_\alpha \to \nu_\beta$ oscillation probabilities for neutrinos and antineutrinos. $V_{eff}(E_\nu)$ is the effective volume of a detector, ρ_{ice} is the ice density, N_A is the Avogadro number, and T is the exposure time.

For the effective mass of the detector we take [9]

$$\rho_{ice} V_{eff}(E_\nu) = 14.6 \times [\log(E_\nu/\text{GeV})]^{1.8} \text{ Mt}.$$

We keep the same effective volume as in [9] in spite of several recent reevaluations for two reasons: (i) for easier comparison of results with those in [9] and some other publications, and (ii) because the final configuration of the detectors are not yet determined. If the effective volume (which also depends on the criteria of selection of events) is reduced by factor of 3–4, the significance for the same exposure period will be reduced by a factor of 1.7–2.0.

Expressions for the inverted mass hierarchy are obtained with substitution NH $\to$ IH. Recall that in the 2ν approximation, when effects of 1–2 mixing and mass splitting are neglected, there are relations between the probabilities for normal and inverted hierarchies

$$P_{\alpha\beta}^{NH} = \bar P_{\alpha\beta}^{IH}, \qquad P_{\alpha\beta}^{IH} = \bar P_{\alpha\beta}^{NH}. \quad (15)$$

That is, an inversion of the mass hierarchy is equivalent to switching neutrinos and antineutrinos. In the three neutrino mixing context, the relations (15) are not exact (see, e.g., Fig. 2 in [9]), especially for the core crossing trajectories.

III. IMPACT OF INELASTICITY DETERMINATION: QUALITATIVE PICTURE

A. Inelasticity and separation of neutrino and antineutrino signals

The hierarchy asymmetries in the neutrino and antineutrino channels have opposite signs. In fact, in the

expressions for the difference of numbers of events for NH and IH (see [9]) all the terms are proportional to the factors $(1 - \kappa_\mu)$ and $(1 - \kappa_e)$, where

$$\kappa_\mu \equiv \frac{\bar{\sigma}^{CC}\bar{\Phi}^0_\mu}{\sigma^{CC}\Phi^0_\mu}$$

is the ratio of cross sections and fluxes of the muon antineutrinos and neutrinos at the production, and κ_e is defined similarly. The ratios κ_μ and κ_e depend on neutrino energy and direction and equal approximately 0.4–0.6. The ν and $\bar{\nu}$ contributions to the number of events partially cancel each other. So, in this case the MH determination relies on the nonequal ν and $\bar{\nu}$ fluxes and cross sections. The separation of the neutrino and antineutrino signals allows us to further reduce the cancellation and therefore to enhance the significance. As follows from Eqs. (11) and (12), the average value of y is 50% larger for ν than for $\bar{\nu}$. Therefore we can use the inelasticity to separate the ν and $\bar{\nu}$ signals.

One possible procedure is to determine for each bin (a large number of events will allow us to do this) the fraction of neutrino and antineutrino events by fitting its y distribution:

(1) Select small enough bins in the neutrino energy-zenith angle plane, so that the oscillatory structures due to certain mass hierarchy are not averaged out (the bin size should be eventually optimized). The number of neutrino and antineutrino events in each bin equals

$$N_{\bar{\nu}} = N\alpha \qquad N_\nu = N(1 - \alpha), \qquad (16)$$

where α is the fraction of antineutrino events and we have omitted the bin indices.

(2) Measure the y distribution of these events.

(3) Fit the measured distribution with

$$p_{\nu\bar{\nu}}(y, \alpha) = (1 - \alpha)p_\nu(y) + \alpha p_{\bar{\nu}}(y), \qquad (17)$$

where $p_\nu(y)$ and $p_{\bar{\nu}}(y)$ are given in (11) and (12), thus, determining the fraction α.

A possible enhancement of the sensitivity to the hierarchy due to the separation of the ν and $\bar{\nu}$ signals can be estimated in the following way. In the described procedure there are two independent observables: the total number of events, $N = N_\nu + N_{\bar{\nu}}$, and α extracted from the y distribution with the accuracy $\delta\alpha$. In general,

$$\delta\alpha \approx \frac{\gamma}{\sqrt{N}}, \qquad (18)$$

where $\gamma = \gamma(\alpha, N)$. The error $\delta\alpha$ can be estimated using the method of moments. As we have two parameters, α and $\delta\alpha$, to extract, it is sufficient to calculate the first and second y moments of $p_{\nu\bar{\nu}}(y, \alpha)$ given in Eq. (17). Using expressions (11) and (12), we obtain the average inelasticity $\langle y \rangle$:

$$\langle y(\alpha) \rangle = \int y p_{\nu\bar{\nu}}(y, \alpha) dy \approx 0.494 - 0.174\alpha. \qquad (19)$$

The mean deviation $\sigma^2_{\bar{y}} \equiv \langle(\bar{y} - \langle y \rangle)^2\rangle$ of the average $\bar{y}$ value after N measurements from the true value $\langle y \rangle$ is

$$\sigma_{\bar{y}}(\alpha, N)^2 = \frac{\sigma_y(\alpha)^2}{N} = \frac{1}{N}\left[\int y^2 p_{\nu\bar{\nu}}(y, \alpha) dy - \langle y(\alpha) \rangle^2\right]$$

$$\approx \frac{1}{N}(0.084 + 0.010\alpha - 0.030\alpha^2). \qquad (20)$$

From Eq. (19) and following a measurement of $\bar{y}$, we obtain a measured value $\tilde{\alpha}$. The average value $\delta\alpha$ is given by

$$\delta\alpha = \sqrt{\langle(\tilde{\alpha} - \alpha)^2\rangle} = \frac{\sqrt{\langle(\bar{y} - \langle y \rangle)^2\rangle}}{0.174} = 5.75\sqrt{\sigma^2_{\bar{y}}}. \qquad (21)$$

Substituting $\sigma^2_{\bar{y}}$ from Eq. (20), we obtain

$$\delta\alpha(\alpha, N) \approx \frac{\gamma}{\sqrt{N}}\sqrt{1 + 0.115\alpha - 0.362\alpha^2}, \qquad (22)$$

where $\gamma = 1.66$.

If α is not close to 1 (for all practical purposes $\alpha \lesssim 0.5$), $\delta\alpha$ weakly depends on α and we can use Eq. (18).

A detailed investigation of $\delta\alpha(\alpha, N)$ by means of the maximum likelihood method confirms the estimate Eq. (22) for large N. For $N \lesssim 100$, this method shows a slight improvement with increasing α with respect to the method of moments. It is worthwhile to further explore this approach.

Let us find the errors σ_ν and $\sigma_{\bar{\nu}}$ in the determination of N_ν and $N_{\bar{\nu}}$. According to Eq. (16), variations of N_ν can be written as

$$\delta N_\nu = (1 - \alpha)\delta N - N\delta\alpha = (1 - \alpha)\sqrt{N} - N\delta\alpha.$$

The variations δN and $\delta\alpha$ are independent and therefore they sum up squared:

$$\sigma^2_\nu = (1 - \alpha)^2 N + (\delta\alpha)^2 N^2,$$
$$\sigma^2_{\bar{\nu}} = \alpha^2 N + (\delta\alpha)^2 N^2. \qquad (23)$$

Assuming that the measured quantities $\tilde{N}$ and $\tilde{\alpha}$ are respectively distributed according to Poisson with mean N and Gaussian with mean α, and standard deviation $\delta\alpha$, the exact variance calculation of $N_{\nu,\bar{\nu}}(\tilde{\alpha}, \tilde{N})$ leads to the same result as in Eq. (23), provided that $N \gg \gamma^2$.

Using (18), we have for NH

$$\frac{\sigma_\nu}{\sqrt{N^{NH}}} = \sqrt{(1 - \alpha)^2 + \gamma^2}, \qquad \frac{\sigma_{\bar{\nu}}}{\sqrt{N^{NH}}} = \sqrt{\alpha^2 + \gamma^2}. \qquad (24)$$

The hierarchy asymmetries in the neutrino and antineutrino channels can then be written as

$$S_\nu = \frac{N^{IH}_\nu - N^{NH}_\nu}{\sigma_\nu}, \qquad S_{\bar{\nu}} = \frac{N^{IH}_{\bar{\nu}} - N^{NH}_{\bar{\nu}}}{\sigma_{\bar{\nu}}}. \qquad (25)$$

Here we assume that NH is the true hierarchy and therefore the corresponding number of events is what is measured.

If $S_{\bar{\nu}}$ and S_{ν} are independent, the total significance equals

$$S_{\text{tot}}^{\text{sep}} = \sqrt{S_{\nu}^2 + S_{\bar{\nu}}^2}.$$

It can be rewritten using Eqs. (25) and (24) as

$$S_{\text{tot}}^{\text{sep}} = \frac{1}{\sqrt{N^{\text{NH}}}} \sqrt{\frac{(N_{\nu}^{\text{IH}} - N_{\nu}^{\text{NH}})^2}{(1-\alpha)^2 + \gamma^2} + \frac{(N_{\bar{\nu}}^{\text{IH}} - N_{\bar{\nu}}^{\text{NH}})^2}{\alpha^2 + \gamma^2}}.$$

For the significance without $\nu - \bar{\nu}$ separation we would have

$$|S_{\text{tot}}| = \left| \frac{N_{\nu}^{\text{IH}} + N_{\bar{\nu}}^{\text{IH}} - N_{\nu}^{\text{NH}} - N_{\bar{\nu}}^{\text{NH}}}{\sqrt{N^{\text{NH}}}} \right|.$$

Therefore the enhancement factor $R \equiv S_{\text{tot}}^{\text{sep}}/|S_{\text{tot}}|$ due to separation of the neutrino and antineutrino signals equals

$$R = \frac{1}{1 - \kappa_{\mu} f_P} \frac{1}{\sqrt{\alpha^2 + \gamma^2}} \sqrt{\frac{\alpha^2 + \gamma^2}{(1-\alpha)^2 + \gamma^2} + (\kappa_{\mu} f_P)^2}. \tag{26}$$

Here

$$\kappa_{\mu} f_P = -\frac{N_{\bar{\nu}}^{\text{IH}} - N_{\bar{\nu}}^{\text{NH}}}{N_{\nu}^{\text{IH}} - N_{\nu}^{\text{NH}}},$$

and

$$f_P \equiv \frac{\bar{P}_{\mu\mu}^{\text{NH}} - \bar{P}_{\mu\mu}^{\text{IH}} + \frac{1}{\bar{r}}(\bar{P}_{e\mu}^{\text{NH}} - \bar{P}_{e\mu}^{\text{IH}})}{P_{\mu\mu}^{\text{IH}} - P_{\mu\mu}^{\text{NH}} + \frac{1}{r}(P_{e\mu}^{\text{IH}} - P_{e\mu}^{\text{NH}})}.$$

If $\bar{r} = r$, in the 2ν approximation we would have $f_P = 1$.

In Eq. (26) the minus sign in the denominator of the first factor reflects the partial cancellation of the hierarchy asymmetries from the neutrino and antineutrino channels. The second factor describes the reduction of enhancement due to the error in the separation of the neutrino and antineutrino signals. The expression is valid if α is not very close to 0 or 1.

Notice that the enhancement factor R does not depend explicitly on the number of events. The number of events is mainly encoded in $\kappa_{\mu} f_P$ and in γ. The value of α changes from bin to bin. For $\alpha = 0.50$ (0.32), $\kappa_{\mu} = 0.4$, and $f_P = 1$ we obtain $R = 1.05$ (1.01).

The enhancement factor is very close to unity. However, a slight improvement on the determination of γ leads to a substantial increase of R. A 10% decrease of γ leads to $R = 1.15$ (1.10) for $\alpha = 0.50$ (0.32).

Notice that according to (25), the ratio

$$\frac{S_{\bar{\nu}}}{S_{\nu}} = -f_p \kappa_{\mu} \frac{\sigma_{\nu}}{\sigma_{\bar{\nu}}}$$

is negative and ν and $\bar{\nu}$ asymmetries have opposite signs.

For ideal separation, $\gamma = 0$, we would have

$$R = \frac{1}{1 - \kappa_{\mu} f_P} \frac{1}{\alpha} \sqrt{\frac{\alpha^2}{(1-\alpha)^2} + (\kappa_{\mu} f_P)^2}.$$

It gives $R = 3.6$ (3.2) for $\alpha = 0.50$ (0.32). This number can be considered as the maximal possible enhancement.

Notice that the estimations presented above differ from the estimations in the case in which the numbers of ν_{μ} and $\bar{\nu}_{\mu}$ events are measured independently (in our previous consideration these numbers correlate). In the latter, $\sigma_{\nu} = \sqrt{N_{\nu}}$, $\sigma_{\bar{\nu}} = \sqrt{N_{\bar{\nu}}}$, and the enhancement factor equals

$$R = \frac{1}{1 - \kappa_{\mu} f_P} \frac{1}{\sqrt{\alpha}} \sqrt{\frac{\alpha}{1-\alpha} + (\kappa_{\mu} f_P)^2}.$$

If $f_P = 1$ and $\kappa_{\mu} \approx 0.5$, we obtain $R = 2.4$ for $\alpha = 0.32$.

The above estimations have been done for a single bin and one should average the enhancement factor over all the bins. Since R depends weakly on N, the estimation for $\alpha \sim 0.5$ gives a good idea about the overall enhancement.

Notice that the weak enhancement factor we obtain is due to the error of the separation parameter, $\delta\alpha$. This is confirmed by exact computations in Sec. V.

B. Inelasticity and reconstruction of neutrino direction

The dominant source of sensitivity loss for the determination of the neutrino mass hierarchy follows from the angular smearing of the oscillograms [9], and in particular, the kinematical smearing due to the angle between the neutrino and muon directions. Indeed, according to (5),

$$\sin^2 \frac{\beta}{2} \approx \frac{Q^2}{4E_{\nu} E_{\mu}} \approx \frac{m_N x y}{2 E_{\mu}}. \tag{27}$$

From this relation with $\langle x \rangle \approx 0.3$ we find that the average angle which characterizes the kinematical smearing is

$$\langle \beta \rangle \approx \frac{0.75}{\sqrt{E_{\nu}/\text{GeV}}} \sqrt{\frac{y}{1-y}}. \tag{28}$$

Then for the average values $y_{\nu} \approx 0.5$ and $y_{\bar{\nu}} \approx 0.3$ it equals $\langle \beta_{\nu} \rangle \approx 0.75/\sqrt{E_{\nu}/\text{GeV}}$ and $\langle \beta_{\bar{\nu}} \rangle \approx 0.5/\sqrt{E_{\nu}/\text{GeV}}$. Using these estimations we find that Δc_{ν} is larger than the region of the same sign hierarchy asymmetry for $E_{\nu} < 6$ GeV.

According to (27), interactions with small y correspond to small scattering angles. Thus, the selection of events with small y reduces the interval of possible values of β. For instance, for a sample with $y < 0.3$, the average inelasticity is about $\langle y \rangle \approx 0.14$. Then according to (28) the average angle between the muon and neutrino incoming directions equals $\langle \beta \rangle \approx 0.13/\sqrt{E_{\nu}/\text{GeV}}$. The sample however retains about 30% of neutrino and 55% of antineutrino events, thus having lower statistics.

At small y, the angular reconstruction error of the muon itself is small, as the muon carries most of the neutrino energy and there are fewer hits from the cascade, which otherwise worsen the reconstruction of the muon direction.

However, at small y, the difference of cross sections of neutrinos and antineutrinos becomes smaller (they are equal at $y = 0$). Therefore the separation of the neutrino and antineutrino signal becomes difficult, and the cancellation of neutrino and antineutrino signals in the hierarchy asymmetry becomes stronger.

For large y, on the other hand, the contribution of $\bar{\nu}$ is strongly suppressed, which eliminates the $\nu - \bar{\nu}$ cancellation. But for events with large y the reconstruction of the neutrino direction is very poor. Furthermore, identification of the ν_μ events becomes difficult (see below).

C. Inelasticity, systematic errors, and degeneracy of parameters

In [9], the method is mainly based on the differential measurement of the neutrino-induced muon flux from different incoming directions and at various energies, avoiding some sources of systematic uncertainties (especially the correlated ones). The approach adopted in this paper goes a step beyond with the additional sensitivity to the $\nu_\mu - \bar{\nu}_\mu$ admixture, or y, providing the method an even stronger immunity to sources of systematic uncertainties.

The degeneracy of the neutrino parameters reduces significantly the sensitivity to the mass hierarchy [9]. The problem may be alleviated, but not avoided, in the future by more precise measurement of neutrino parameters in MINOS, T2K, NOvA, and in reactor experiments. The use of inelasticity in analyses will reduce the impact of degeneracies. Indeed, effects of uncertainties, e.g. in Δm_{32}^2 and θ_{23}, are nearly the same for ν and $\bar{\nu}$, while the y distributions for ν and $\bar{\nu}$ are different. Therefore measurements of inelasticity will allow us to somehow separate the effects. A quantitative study of the corresponding improvements will be given in Sec. V.

D. Inelasticity and identification of ν_μ events

As discussed in [9], tau neutrinos contaminate the ν_μ sample by about 5% contribution. The oscillation effect on this contribution differs from the one on the true ν_μ events. This leads to a kind of additional smearing, which cannot be neglected. The inelasticity observable enables us to further suppress the number of $\nu_\tau \to \mu$ events in a sample because of the specific vertex kinematics of tau neutrino interactions: rather large showers are produced and the angle between the muon and tau neutrino is large, as the muon is sharing energy with two other neutrinos. Therefore this class of events has on average a rather large effective y, and restricting an analysis to small y will allow us to disentangle at least partly the ν_τ contribution. Quantitative analysis of this suppression is beyond the scope this paper.

For large y, due to the low energy of the muons, the probability of misidentification of the ν_μ events with the CC $\nu_{e,\tau}$ events as well as the NC events of all neutrino species becomes large. Indeed, there can be confusion between the charged pions and muons as they both have a long decay length ($\lambda_{\pi^\pm} \approx 56$ m at 1 GeV) and propagate with low energy loss rate (the dominant ionization energy loss limits their range to $\lesssim 5$ m per GeV). However, the energy distributions of muons and pions strongly differ: the simulation with GENIE [15] of 10 GeV ν_μ interactions shows that the most probable $E_{\pi^\pm}$ is of the order of a few 100 MeV, so that $E_{\pi^\pm} \approx 1$ GeV is already unlikely high. The reaction favors events with higher π multiplicity rather than events with higher π energies.

IV. 3D DISTRIBUTIONS AND OSCILLOGRAMS

As we saw in the previous section the separation of the neutrino and antineutrino signals requires measurements of the y distribution in a wide range of y, and especially for large y, where the difference of the neutrino and antineutrino cross section is maximal. On the other hand, good reconstruction of the neutrino directions requires selection of events with small y. In a sense, improvements of the sensitivity due to $\nu - \bar{\nu}$ separation and narrowing the angular distribution are incompatible. Small y's are preferred also for the identification of the ν_μ events and the disentanglement of the ν_μ from $\nu_{e,\tau}$ events. Therefore, one expects that the best sensitivity to the neutrino mass hierarchy is for the intermediate range of y. Here the interplay of different effects occurs, which requires a combined description using the differential characteristics in y and also in x since the angle depends on x too.

A. Densities of events: Oscillograms for different y

The density of the ν_μ events as a function of E_ν, c_μ, y equals

$$n_\nu^{\mathrm{NH}}(E_\nu, c_\mu, y) = \frac{1}{2\pi} \int_{c_\beta^{\min}}^1 dc_\beta \int_0^{2\pi} d\phi \frac{d^2 \sigma_\nu^{\mathrm{CC}}}{dc_\beta dy}$$
$$\times \frac{\rho_\nu^{\mathrm{NH}}(E_\nu, c_\nu)}{\sigma_\nu^{\mathrm{CC}}(E_\nu)},$$

where ρ_ν^{NH} is defined in (13), c_ν is given in (7), and the lower limit of integration $c_\beta^{\min}$ is defined in (6). Similar expressions can be written for antineutrinos and for the IH case.

Using the relation Eq. (7), we change the integration variables, $d\phi \to dc_\nu$:

$$n_\nu^{\mathrm{NH}}(E_\nu, c_\mu, y) = \frac{1}{\pi} \int_{c_\beta^{\min}}^1 dc_\beta \frac{d^2 \sigma_\nu^{\mathrm{CC}}}{dc_\beta dy}(x(c_\beta), y)$$
$$\times \int_{c_\nu^{\min}}^{c_\nu^{\max}} dc_\nu \frac{1}{\sqrt{h(c_\mu, c_\beta, c_\nu)}} \frac{\rho_\nu^{\mathrm{NH}}(E_\nu, c_\nu)}{\sigma_\nu^{\mathrm{CC}}(E_\nu)}.$$
$$(29)$$

Here

$$h \equiv (s_\mu s_\beta)^2 - (c_\nu - c_\mu c_\beta)^2,$$

and $1/\sqrt{h}$ is essentially the Jacobian of transition to new variables according to (7). The limits of integration $c_\nu^{\max}$ and $c_\nu^{\min}$ will be specified later. Notice that appearance of an additional factor 2 in the expression (29) is due to twofold ambiguity at the transition from ϕ to c_ν.

Let us make another change of the integration variable: $c_\beta \rightarrow x$. Using the equality

$$\frac{d^2\sigma_\nu^{\text{CC}}}{dc_\beta dy} dc_\beta = \frac{d^2\sigma_\nu^{\text{CC}}}{dx dy} dx,$$

we obtain from (29)

$$n_\nu^{\text{NH}}(E_\nu, c_\mu, y) = \frac{1}{\pi} \int_{x_{\min}}^{x_{\max}} dx \int_{c_\nu^{\min}}^{c_\nu^{\max}} dc_\nu \frac{d^2\sigma_\nu^{\text{CC}}}{dx dy}$$
$$\times \frac{1}{\sqrt{h(c_\mu, c_\beta, c_\nu)}} \frac{\rho_\nu^{\text{NH}}(E_\nu, c_\nu)}{\sigma_\nu^{\text{CC}}(E_\nu)}.$$

Here $x_{\min,\max}$ correspond to the values $c_\beta(E_\nu, x, y) = \pm 1$. In turn, the limits of integration over c_ν correspond to $h = 0$, i.e., to the borders of the interval of the positivity condition: $h \geq 0$. Indeed, the expression for h can be rewritten as

$$h = -[c_\nu - \cos(\theta_\mu - \beta)] \times [c_\nu - \cos(\theta_\mu + \beta)],$$

where $\beta = \beta(x, y, E_\nu)$ is determined in Eq. (4). Then the limits $c_\nu^{\max} = \cos(\theta_\mu - \beta)$ and $c_\nu^{\min} = \cos(\theta_\mu + \beta)$ follow immediately.

Changing the order of integrations over x and c_β, we obtain

$$n_\nu^{\text{NH}}(E_\nu, c_\mu, y)$$
$$= \frac{1}{\pi} \int_{|\theta_\mu - \theta_\nu| \leq \beta_0} dc_\nu \rho_\nu^{\text{NH}}(E_\nu, c_\nu) g_\nu(E_\nu, y, c_\nu, c_\mu), \quad (30)$$

where

$$g_\nu(E_\nu, y, c_\nu, c_\mu) \equiv \frac{1}{\sigma_\nu^{\text{CC}}(E_\nu)} \int_{x^-}^{x^+} dx \frac{d^2\sigma_\nu^{\text{CC}}(E_\nu, x, y)}{dx dy}$$
$$\times \frac{1}{\sqrt{s_\beta^2 s_\mu^2 - (c_\nu - c_\beta c_\mu)^2}}. \quad (31)$$

Here s_β and c_β are functions of E_ν, x, and y. The function g_ν does not depend on the mass hierarchy and essentially plays the role of the kinematic smearing function.

Writing similar expressions for IH and $\bar{\nu}$, we obtain the densities of the events for NH and IH:

$$n^{\text{NH,IH}}(E_\nu, c_\mu, y)$$
$$= n_\nu^{\text{NH,IH}}(E_\nu, c_\mu, y) + n_{\bar{\nu}}^{\text{NH,IH}}(E_\nu, c_\mu, y)$$
$$= \frac{1}{\pi} \int_{|\theta_\mu - \theta_\nu| \leq \beta_0} dc_\nu [\rho_\nu^{\text{NH,IH}}(E_\nu, c_\nu) g_\nu(E_\nu, y, c_\nu, c_\mu)$$
$$+ \rho_{\bar{\nu}}^{\text{NH,IH}}(E_\nu, c_\nu) g_{\bar{\nu}}(E_\nu, y, c_\nu, c_\mu)]. \quad (32)$$

Introducing $\rho^{\text{NH}} \equiv \rho_\nu^{\text{NH}} + \rho_{\bar{\nu}}^{\text{NH}}$, we can rewrite the expression in (32) as

$$n^{\text{NH}}(E_\nu, c_\mu, y)$$
$$= \frac{1}{\pi} \int_{|\theta_\mu - \theta_\nu| \leq \beta_0} dc_\nu \rho^{\text{NH}}(E_\nu, c_\nu) G(E_\nu, y, c_\nu, c_\mu),$$

where

$$G(E_\nu, y, c_\nu, c_\mu) \equiv g_\nu \frac{\rho_\nu^{\text{NH}}}{\rho^{\text{NH}}} + g_{\bar{\nu}} \frac{\rho_{\bar{\nu}}^{\text{NH}}}{\rho^{\text{NH}}}.$$

The function G can be immediately compared with the Gaussian smearing function, which was used in [9] embedding both kinematic and experimental resolution effects.

Let us find the limits of integration over x in Eq. (31). According to Eq. (5)

$$x(c_\beta) = \frac{2E_\nu(E_\mu - |\mathbf{p}_\mu|c_\beta) - m_\mu^2}{2m_N E_\nu y},$$

which imposes the lower and upper bounds to x:

$$x^\pm = x(\cos(\theta_\nu \pm \theta_\mu)).$$

For a given θ_ν and θ_μ, the minimal angle between the muon and the neutrino is $\beta = |\theta_\mu - \theta_\nu|$. The maximal angle β is given by $c_{\beta,\max} = \cos(\theta_\nu + \theta_\mu)$.

The integration over c_ν in Eq. (30) runs from $\cos(\theta_\mu + \beta_0)$ to $\cos(\theta_\mu - \beta_0)$, where $c_{\beta_0} = c_\beta(E_\nu, x = 1, y)$ and $\theta_\mu \pm \beta_0$ is restricted by the interval $0 - \pi$.

B. Kinematical smearing function

According to Eq. (30), the functions $g_{\nu,\bar{\nu}}(E_\nu, y, c_\nu, c_\mu)$ in (31) can be considered as the smearing functions over the neutrino angle. Figure 1 shows dependence of g_ν and $g_{\bar{\nu}}$ on c_μ for several values of c_ν and y.

The smearing functions differ from the Gaussian function assumed in [9]. They have two peaks with a local minimum in between; there are no exponential tails; the central parts are at $c_\mu \approx c_\nu$. The asymmetry of the peaks becomes stronger with c_μ approaching ± 1; the width of the functions increases with y. The functions g are similar for neutrinos and antineutrinos. As expected, for antineutrinos the overall normalization decreases with the increase of y, whereas for neutrinos normalization changes weakly.

The properties of $g_{\nu,\bar{\nu}}$ can be readily understood from the expression for h. Indeed, $g_{\nu,\bar{\nu}}$ have inverted (and also smoothed) shapes with respect to that of $\sqrt{h}$. In particular,

peaks of $g_{\nu,\bar{\nu}}$ correspond to zeros of h, the minima of $g_{\nu,\bar{\nu}}$ correspond to the maxima of h, etc.

The function h can be rewritten as

$$h = s_\beta^2 - (c_\nu^2 + c_\mu^2) + 2c_\nu c_\mu c_\beta,$$

which is obviously symmetric with respect to the interchange

$$c_\nu \leftrightarrow c_\mu.$$

As a consequence, $g_{\nu,\bar{\nu}}$ also obeys this symmetry.

Introducing

$$r \equiv 2\zeta xy = 2\sin^2\frac{\beta}{2},$$

we can present h as

$$h = 2r(1 - c_\nu c_\mu) - r^2 - (c_\nu - c_\mu)^2.$$

Then defining the difference $\Delta \equiv c_\nu - c_\mu$, we have

$$h(\Delta) = s_\mu^2(2r - r^2) - (\Delta + rc_\mu)^2.$$

So, h, as function of Δ, is an inverted parabola with its maximum shifted to $\Delta = -rc_\mu$. In agreement with Fig. 1, $h(\Delta)$ is not symmetric with respect to $\Delta = 0$ or $c_\nu = c_\mu$, and the minimum of $g_{\nu,\bar{\nu}}$ is shifted with respect to $c_\mu = c_\nu$. This also leads to a difference in the heights of the peaks.
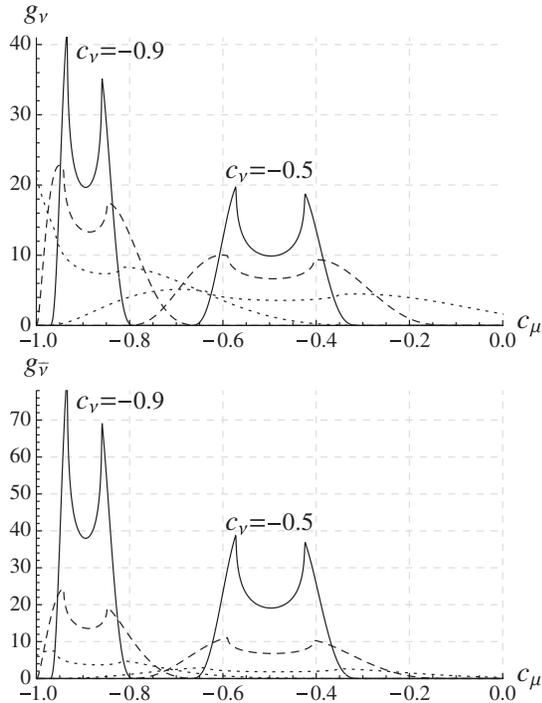

FIG. 1. The angular smearing functions for neutrinos (upper panel) and antineutrinos (bottom panel) for $E_\nu = 10$ GeV and different values of c_ν (numbers at the curves). Solid, dashed, and dotted curves are respectively for $y = 0.2$, $y = 0.5$, and $y = 0.8$.

Zeroes of h are at

$$\Delta = -rc_\mu \pm \sqrt{s_\mu^2(2r - r^2)}.$$

According to (8), in terms of angles, the zeros of h are given by $\cos\theta_\nu = \cos(\theta_\mu \pm \beta)$. So, the width of the smearing function increases with β. In turn, according to (28), $\beta \propto \sqrt{y}$, and consequently, the width increases with y, as we mentioned before.

It is easy to understand the appearance of peaks in $g_{\nu,\bar{\nu}}(c_\nu)$ at the borders of the allowed interval using the following graphical representation. The neutrino vector is on the surface of the cone with angle β and axis along the muon momentum. With change of ϕ, the neutrino vector moves on the surface of the cone. The maximum and minimum of c_ν given by (8) correspond to the neutrino vector situated in the plane formed by the muon vector and the axis z and the neutrino vector is moving perpendicularly to this plane. Therefore around these positions the z projection of the neutrino vector does not change appreciably, and so the integration over ϕ leads to bigger contribution.

C. Oscillograms for different values of y

We will use the general formulas obtained in the previous sections to compute the oscillograms and asymmetry distributions for different values of y. The functions $\rho_{\nu,\bar{\nu}}^{NH,IH}(E_\nu, c_\nu)$ are taken from [9].

Figure 2 shows the $E_\nu - \cos\theta_\mu$ binned distribution of the hierarchy asymmetry with the inelasticity (y dependence) and kinematical smearing taken into account. Different panels in this figure correspond to different y intervals $\{y_{\min}, y_{\max}\}$. The asymmetry in these intervals has been computed in the following way. We first used very small y bins $\Delta y \ll (y_{\max} - y_{\min})$. We computed the asymmetry in each of these small bins $S_k = S(y_k, E_\nu, \cos\theta_\mu)$ and then the total asymmetry in the interval $\{y_{\min}, y_{\max}\}$ as $S_{tot} = \sqrt{\sum S_k^2}$ (the sum runs over all small y bins in the interval $\{y_{\min}, y_{\max}\}$), and the sign is the same as for the dominant contribution. In practice the summation over small bins was substituted by integration:

$$S(y_{\max}, y_{\min}, E_\nu, \cos\theta_\mu) = \left[\int_{y_{\min}}^{y_{\max}} dy \frac{(n^{IH} - n^{NH})^2}{n^{NH}}\right]^{1/2}.$$

Here $n^{NH,IH}$ is the number of events in the bin $\Delta E_\nu \Delta \cos\theta_\mu$ given in (32).

The first panel of Fig. 2 corresponds to $\{y_{\min}, y_{\max}\} = \{0, 1\}$, the others to various intervals with $y_{\max} - y_{\min} = 0.2$. The first panel is the sum of contributions described in other panels. As we see, the biggest contribution comes from the intermediate region $y \in \{0.3, 0.7\}$. Indeed, at small y the hierarchy asymmetry is suppressed due to strong cancellation of the nearly equal contributions from
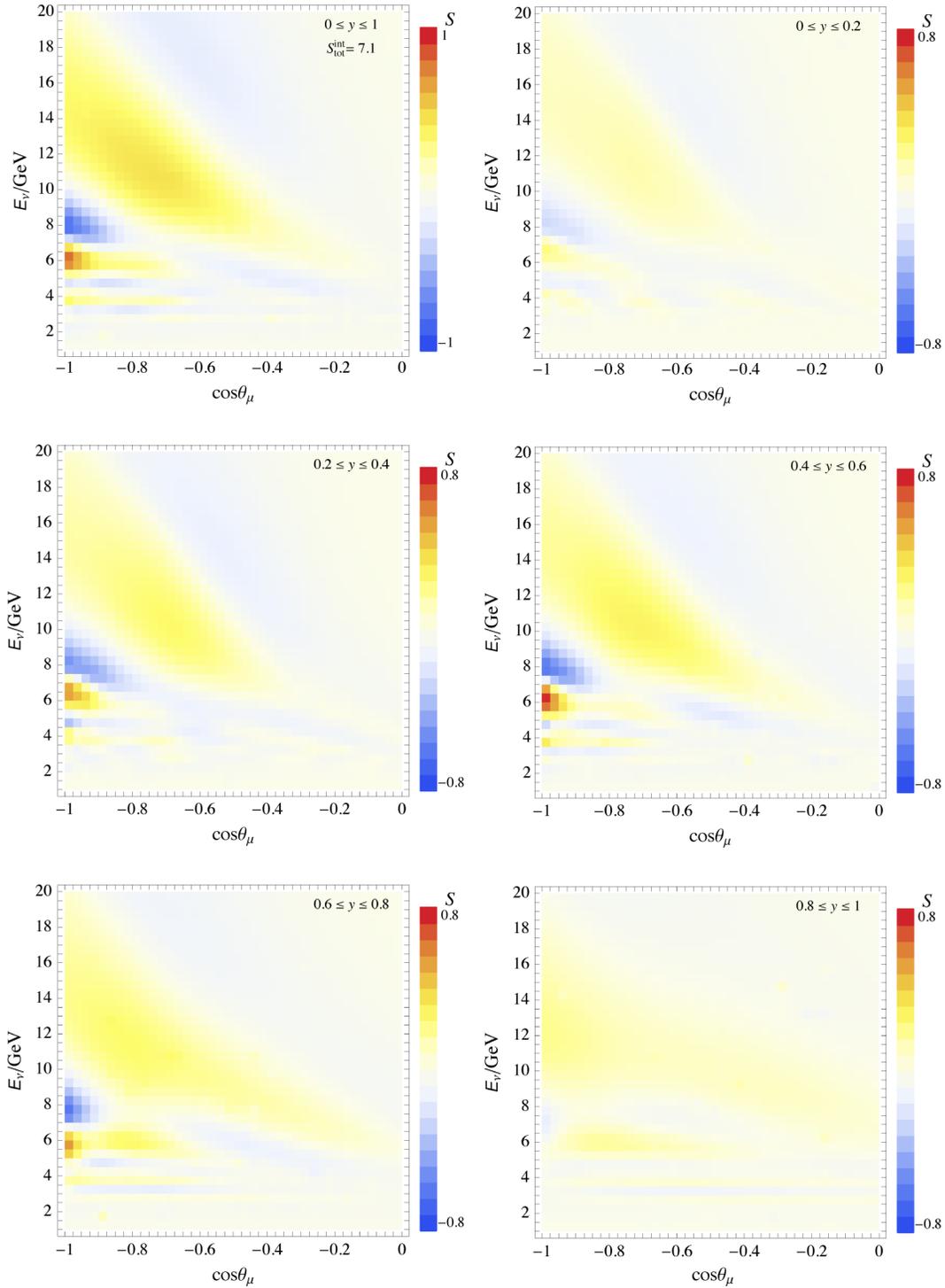
FIG. 2 (color online).   The hierarchy asymmetry distributions after the kinematical smearing for various inelasticity ranges and for one year of exposure.

neutrinos and antineutrinos (recall that at $y \sim 0$ the ν and $\bar{\nu}$ cross sections become equal). At large y, the asymmetry is suppressed due to strong smearing over the angle between muon and neutrino. With the increase of y, the region of strong asymmetry first shifts smaller E_ν and larger $\cos\theta_\mu$, and then move to larger E_ν and $\cos\theta_\mu = -1$. The region expands in a horizontal ($\cos\theta_\mu$) direction for small y.

The total significance (given by integration over the first panel with $0 \leq y \leq 1$) equals

$$|S_{\text{tot}}| = \left[\int dc_\mu \int dE_\nu \int_0^1 dy \frac{(n^{\text{IH}} - n^{\text{NH}})^2}{n^{\text{NH}}} \right]^{1/2}. \quad (33)$$

For exposure $T = 1$ year, this leads to $|S_{\text{tot}}| = 8.43$.

If the y dependence is not used, the densities of events should be integrated over y before computing S. This gives

$$|S_{\text{tot}}^{\text{int}}| = \left[\int dc_\mu \int dE_\nu \frac{(\int_0^1 dy (n^{\text{IH}} - n^{\text{NH}}))^2}{\int_0^1 dy n^{\text{NH}}} \right]^{1/2}. \quad (34)$$

For one year of exposure we obtain from (34) $|S_{\text{tot}}^{\text{int}}| = 7.11$, which is about 15% smaller than in the case when the y distribution is used according to Eq. (33).

The following comments are in order.

(i) The kinematical smearing strongly reduces the total significance: for the ideal reconstruction of the neutrino energy and direction we would obtain $|S_{\text{tot}}^{\nu+\bar{\nu}}| = 23.7$ in one year even without y information. This number can be considered as a maximal achievable significance. It should be compared with $|S_{\text{tot}}^{\text{int}}| = 7.11$ obtained from (34). Note that $|S_{\text{tot}}| = 8.43$ can be obtained with an ideal detector having perfect resolutions (see Sec. V).

(ii) The increase of significance by about 15% with y distribution is better than the one predicted from our qualitative discussion in Sec. III using γ derived from the method of moments. This is probably related to the fact that the characteristics of the y distribution are more fully exploited.

Note also that in our treatment the cross sections have been restricted to the DIS approximation, and thus exhibit cutoffs at small y, a region of good angular resolution. Therefore a more complete description of the cross sections will recover the events in the small y region, further enhancing the significance.

V. SIGNIFICANCE OF DETERMINATION OF MASS HIERARCHY WITH INELASTICITY

In the previous section we have taken into account the kinematical smearing; the integration over the angle between the neutrino and muon, β. Besides this, one should perform the experimental smearing over the observables: the energy of muon and cascade as well as the direction of muon due to finite experimental energy and angular resolutions.

A. Experimental resolution functions

We present here the significance of the identification of the mass hierarchy, considering various scenarios for the widths $\sigma_{\mu,h}(E_\nu, y)$ and $\sigma_\psi(E_\nu, y)$ of the energy and angular resolution functions. We use the notation $\tilde{x}$ for the reconstructed value of the observable x.

1. Energy resolution

We assume the Gaussian energy resolution functions of the cascade and muon with widths σ_h and σ_μ correspondingly. Then the neutrino energy resolution is itself the Gaussian function (sum of two normal distributions):

$$g_{E_\nu}(\tilde{E}_\nu, E_\nu) = \frac{1}{\sqrt{2\pi}\sigma_{E_\nu}} \exp\left[-\frac{1}{2} \frac{(\tilde{E}_\nu - E_\nu)^2}{\sigma_\nu^2} \right] \quad (35)$$

with width

$$\sigma_\nu(y) = \sqrt{\sigma_\mu^2 + \sigma_h^2},$$

which depends on y.

We consider two cases for the energy resolution of muons and cascades:

(i) $\sigma_{\mu,h} = bE_{\mu,h}$, which gives $\sigma_\mu = bE_\mu \approx b(1-y)E_\nu$ and $\sigma_h = bE_h \approx byE_\nu$, so that

$$\sigma_\nu(y) = bE_\nu\sqrt{1 - 2y + 2y^2};$$

(ii) $\sigma_{\mu,h} = \sqrt{bE_{\mu,h}}$, then

$$\sigma_\nu = \sqrt{bE_\nu},$$

which has the same form as $\sigma_{\mu,h}$. We make here a reasonable simplification that b is the same for cascades and muons. In fact, this is true only if we assume that most of the energy of the cascade is visible like for a muon. More likely, it has a bit smaller Cherenkov photon yield per GeV and is subject to greater event-by-event fluctuations.

In the case (*i*), we use $b = 0.3$ in order to compare with the results from [9]. In the case (*ii*), we take b in the range $0.35 \leq b \leq 0.7$, which is derived from an estimated number of detected photons $n_{\text{hit}}/\text{GeV} \approx 1\text{–}3$ [16]. Equation (26) in [16] predicts $n_{\text{hit}}/\text{GeV} \approx 1.5$ for a mean distance of about 10 m between the Cherenkov light emitter and an optical module of the IceCube type. The range is extended in the mentioned limits, because the precise topology and technology (for instance, the photo-detection efficiency and area of the optical modules) of a dense array are not yet precisely known.

We then obtain the energy resolution given by the statistical uncertainty of the number of expected hits:

$$\sigma_{\mu,h} = \frac{\delta(E_{\mu,h} n_{\text{hit}}/\text{GeV})}{n_{\text{hit}}/\text{GeV}}$$

$$\approx \sqrt{\{0.35, 1\} E_{\mu,h}} \approx \{0.6, 1\}\sqrt{E_{\mu,h}}. \quad (36)$$

2. Inelasticity resolution function

The inelasticity distribution $g_y(E_\nu, y)$ can be derived straightly from $E_{\mu,h}$ distributions, $g_{\mu,h}(\tilde{E}_{\mu,h}, E_{\mu,h})$ described above. We show in Appendix B that it is nearly

Gaussian in most cases of interest. It deviates from Gaussian, showing enhanced tails, when E_μ and E_h are both small. In our computations we use the Gaussian function with width

$$\sigma_y = \frac{1}{\sqrt{2}}\left(\frac{E_h + \sigma_h}{E_h + \sigma_h + E_\mu - \sigma_\mu} - y\right). \quad (37)$$

Notice that we could perform smearing using immediately E_μ and E_h without introducing y, and if needed, introduce $\tilde{y}$ after smearing.

3. Angular resolution

The angle ψ between the true and the reconstructed muon directions is described by the normalized distribution

$$g_\psi = \frac{2\psi}{\sigma_\psi^2}\exp\left(-\frac{\psi^2}{\sigma_\psi^2}\right), \quad (38)$$

which is derived from the 2D Gaussian distribution. The interval $\psi \leq \sigma_\psi$ encloses 63%, and g_ψ peaks at $\sigma_\psi/\sqrt{2}$. The width σ_ψ is generically a function of E_μ, which has the form [13]

$$\sigma_\psi = \psi_0\sqrt{\frac{m_N}{E_\mu}}.$$

Here ψ_0 depends on the detector medium (ice, water) and its topology. The IceCube detector is sparsely instrumenting a medium of relatively short scattering length. Therefore a large number of photons will not travel on a straight path between the Cherenkov light emission point and the detection location. On the contrary in ANTARES (and similarly in ORCA), the photons are detected undelayed. This is the main reason why IceCube has worse angular resolution than the ANTARES detector. Therefore, we consider ψ_0 values in a range reflecting common angular resolutions achieved in water and by a sparse array in ice. Note, however, that one reasonably expects a substantially improved angular resolution in ice with a smaller and denser array (PINGU), i.e., a global reduction of scale: in this case the short scattering length will be of relative importance and many Cherenkov photons will be undelayed in reaching the optical modules that are closest to their emission point.

The angular resolution of an event with 60 hits is about 5° in IceCube and better than 2° ($n_{\rm hit}/{\rm GeV} \approx 1.5$) in ANTARES. Therefore $15° \lesssim \psi_0 \lesssim 30°$. The range $1 \leq n_{\rm hit}/{\rm GeV} \leq 3$ leads to $8.5° \lesssim \psi_0 \lesssim 40°$.

The smearing function for the zenith angle of muon $g(c_\mu, \tilde{c}_\mu)$ can be computed using the smearing function for ψ (38) as

$$g(c_\mu, \tilde{c}_\mu) = \frac{1}{\pi}\int_{|\theta_\mu - \tilde{\theta}_\mu|}^{\pi}\frac{g_\psi(\psi)\mathrm{d}\psi}{\sqrt{\tilde{s}_\mu^2 s_\psi^2 - (\tilde{c}_\mu c_\psi - c_\mu)^2}}. \quad (39)$$
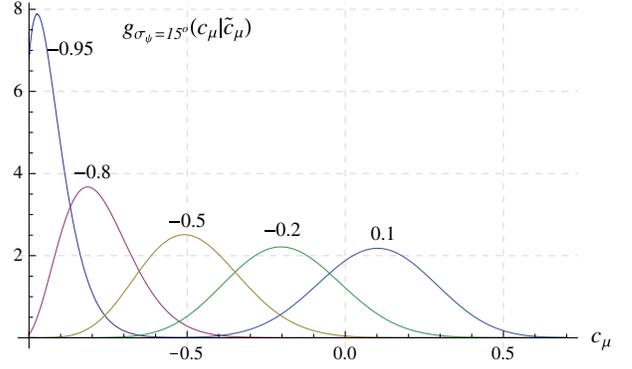

FIG. 3 (color online). Angular smearing function in $\cos\theta_\mu$ for $\sigma_\psi = 15°$ and several values of $\tilde{c}_\mu$.

The denominator here appears similarly to that at the variable change $\phi \to c_\nu$ performed in Eq. (29). The function $g(c_\mu, \tilde{c}_\mu)$ is normalized, which follows from normalization of g_ψ.

Figure 3 shows the angular smearing function $g(c_\mu, \tilde{c}_\mu)$ for $\psi_0 = 15°$ and several values of $\tilde{c}_\mu$. Notice that $g_\psi(c_\mu, \tilde{c}_\mu)\tilde{s}_\mu$ is not symmetric and it increasingly deviates from the normal distribution, when approaching $\theta_\mu = 180°$.

B. Distributions with experimental smearing

We calculate the distribution of events smeared over the experimental resolution functions. We convert the 3D distributions in the parameter space $E_\nu - y - c_\mu$ into observed parameters space $\tilde{\theta}_\mu, \tilde{E}_\nu, \tilde{y}$ convoluting n with the resolution distributions for E_ν, y, and ψ:

$$\hat{n}_{\nu,\bar{\nu}}^{\rm IH,NH}(\tilde{\theta}_\mu, \tilde{E}_\nu, \tilde{y}) = n_{\nu,\bar{\nu}}^{\rm IH,NH}(\theta_\mu, E_\nu, y) * (g_\psi g_y g_\nu).$$

The convolution is performed sequentially in the order indicated in the last brackets. The smearing functions are taken according to Eqs. (35), (39), and (37) (the width of Gaussian function for g_y). Values of $n_{\nu,\bar{\nu}}^{\rm IH,NH}$ outside region $1 < E_\nu/{\rm GeV} < 20$ and for $\theta_\mu < 90°$ are set to the values taken at the boundaries.

Integrating over the bins, we obtain the binned oscillogram:

$$N_{ijk}(\tilde{c}_{\mu i}, \tilde{E}_{\nu j}, \tilde{y}_k) = \int_{\mathrm{bin}(ijk)}\mathrm{d}\tilde{c}_\mu\mathrm{d}\tilde{E}_\nu\mathrm{d}\tilde{y}\,\hat{n}_{\nu,\bar{\nu}}^{\rm IH,NH}(\tilde{\theta}_\mu, \tilde{E}_\nu, \tilde{y}).$$

The smeared distributions in the plane $E_\nu - \cos\theta_\mu$ for different intervals of y and different resolutions are shown in Figs. 4–6.

In comparison with Fig. 2, the overall scale of asymmetries is reduced by a factor of $\sim$2, which quantifies the effect of experimental smearing. The position and shape of the regions of strong asymmetry follow to a large extent those in Fig. 2.
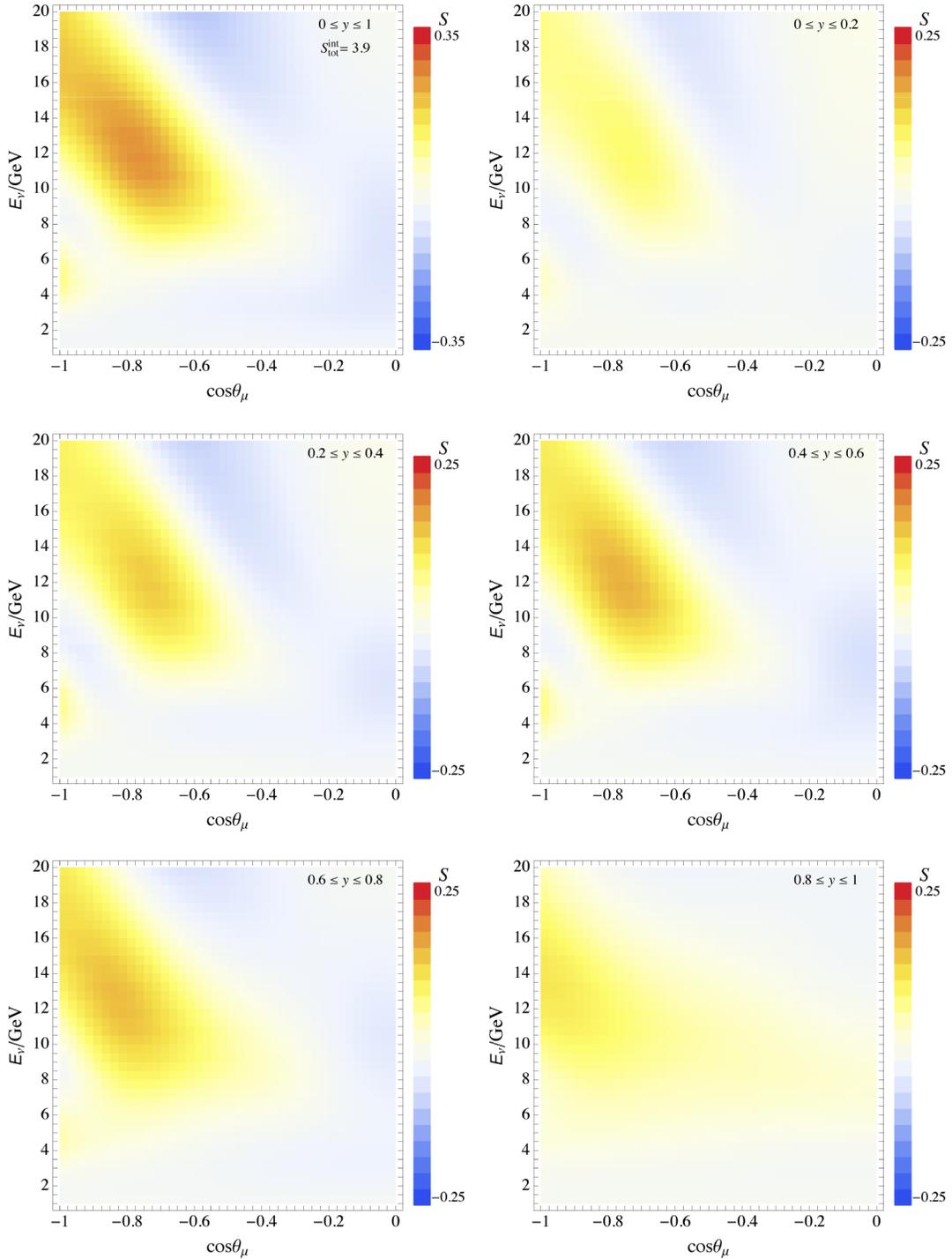
FIG. 4 (color online).   The hierarchy asymmetry distribution in the $(E_\nu - \cos\theta_\mu)$ plane for different intervals of the inelasticity and for one year of exposure. The experimental smearing of the distributions was performed with the energy and angular resolutions $\sigma_E = \sqrt{0.7E}$, $\psi_0 = 20°$.

C. Estimations of the total significance

Total significances with the experimental smearing are calculated using Eqs. (33) and (34) with replacement $n \rightarrow \hat{n}$. Table I presents the total significance after one year of exposure for several experimental resolution

scenarios, including the one with only kinematical smearing.

For comparison we also compute the significances obtained immediately from the neutrino oscillograms, which corresponds to exact reconstruction of the neutrino
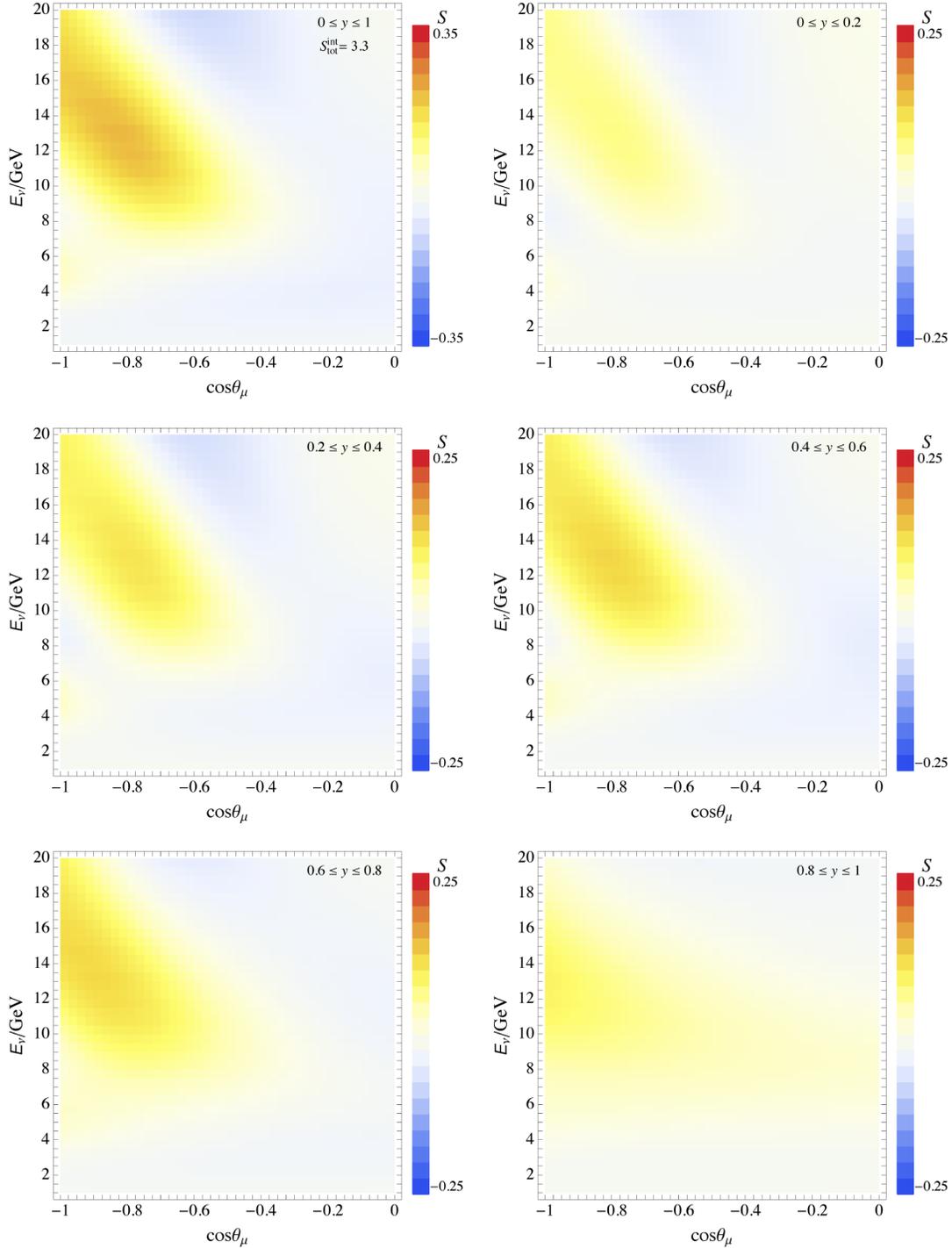
FIG. 5 (color online).   The same as in Fig. 4 with $\sigma_E = \sqrt{0.7E}$ and $\psi_0 = 40°$.

energy and direction. If ν and $\bar{\nu}$ distributions are measured independently, we would have $|S_{\text{tot}}^{\nu}| = 46.8$, $|S_{\text{tot}}^{\bar{\nu}}| = 43.8$, and the total significance $|S_{\text{tot}}| = \sqrt{|S_{\text{tot}}^{\nu}|^2 + |S_{\text{tot}}^{\bar{\nu}}|^2} = 64.1$. The latter is about 3 times larger than the total significance in the case when ν and $\bar{\nu}$ signals are not separated $|S_{\text{tot}}^{\nu+\bar{\nu}}| = 23.7$, in agreement with our qualitative result in Sec. III.

In the realistic case of partial separation of the ν and $\bar{\nu}$ signals, which takes place when y information is included, and after the kinematical smearing the significance decreases strongly down to 8.43 after one year (so that after three years of exposure we would have $|S_{\text{tot}}^{3\,\text{yr}}| = 14.6$). This number further reduces down to $|S_{\text{tot}}^{3\,\text{yr}}| \approx 6.1$
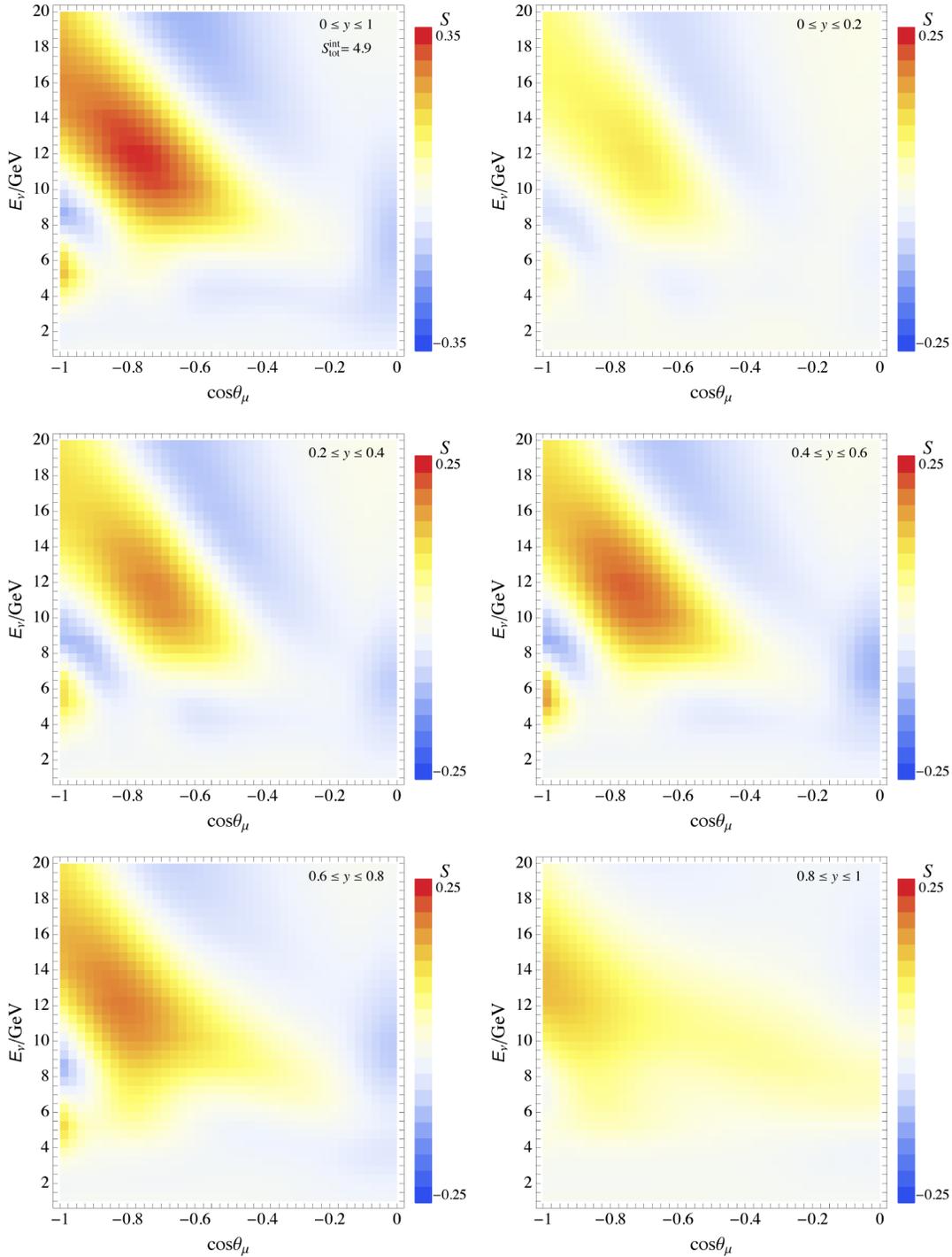
FIG. 6 (color online).　The same as in Fig. [4] with $\sigma_E = \sqrt{0.35E}$ and $\psi_0 = 10°$.

after the experimental smearing in our worst case scenario ($\sigma_{\mu,h} = \sqrt{0.7E_{\mu,h}}$, $\sigma_\psi = 40°$).

Systematic uncertainties likely play a relatively mild role in degrading these results, as the measurements are differential from neighboring locations (bins in E_ν and c_μ), and the systematic uncertainties between neighboring bins with different asymmetries are strongly correlated. In addition, the y distribution must be a superposition of the y distributions of neutrino and of antineutrino events, strongly constraining its shape and providing information related to the systematic effect in the y dimension. However, we have also found negligible degradation of the significance (about 1%) if introduced as in [9], at the level of 10%. This is due to the small bin size of our oscillograms.

TABLE I. The total significance of identification of the neutrino mass hierarchy for different experimental smearing scenarios and for one year of exposure. S_{tot} refers to analysis with inelasticity, whereas $S_{\text{tot}}^{\text{int}}$ refers to the y integrated distributions analysis. The upper line with $\sigma_E = \psi_0 = 0$ corresponds to the kinematical smearing only.

σ_E	ψ_0	$|S_{\text{tot}}|$	$|S_{\text{tot}}^{\text{int}}|$	$|S_{\text{tot}}|/|S_{\text{tot}}^{\text{int}}|$
0	0	8.43	7.11	1.19
$\sqrt{0.35E}$	10°	5.44	4.90	1.11
$\sqrt{0.35E}$	20°	5.10	4.66	1.10
0.3E	20°	4.40	3.98	1.11
$\sqrt{0.7E}$	20°	4.19	3.87	1.08
$\sqrt{0.7E}$	40°	3.52	3.26	1.08

Figure 7 shows the dependence of the significance on the upper limit of integration over y for the case $\sigma_{\mu,h} = \sqrt{0.35E_{\mu,h}}$ and $\psi_0 = 20°$ and for kinematical smearing only. The dashed curves are for y-integrated significances.

According to Fig. 7, the increase of the significance is sustained up to higher y for curves including experimental smearing. This is due to the contribution to the asymmetry from larger E_ν, whose relative importance in smearing decreases. Also the difference between y-differential and y-integrated significances is relatively small after the experimental smearing.

D. Δm_{32}^2 degeneracy

The effect of an inversion of the mass hierarchy (especially at large energies) is rather similar to a shift of the oscillation probabilities in the energy scale (see [9]). This is equivalent to a change of Δm_{32}^2. Therefore the effect of hierarchy can be partly mimicked by a change of Δm_{32}^2. Indeed, the pattern of distribution of the quantity
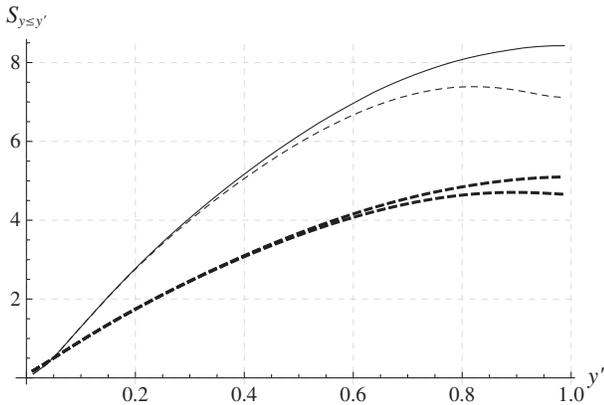

FIG. 7. Dependence of the significance on the upper limit of integration over y. Thin and thick curves respectively correspond to kinematical smearing only and to experimental smearing included. Solid and dashed curves respectively show S_{tot} and $S_{\text{tot}}^{\text{int}}$.

$$S^\delta \equiv \frac{N^{\text{NH}}(\Delta m_{32}^2 + \delta) - N^{\text{NH}}(\Delta m_{32}^2)}{\sqrt{N^{\text{NH}}(\Delta m_{32}^2)}} \qquad (40)$$

in the $E_\nu - c_\mu$ plane is rather similar for certain values of the shift parameter, δ, to the hierarchy asymmetry pattern:

$$S^{\text{MH}} \equiv \frac{N^{\text{IH}}(\Delta m_{32}^2) - N^{\text{NH}}(\Delta m_{32}^2)}{\sqrt{N^{\text{NH}}(\Delta m_{32}^2)}}. \qquad (41)$$

Since Δm_{32}^2 is known with some error, this parameter degeneracy degrades the sensitivity to the mass hierarchy. To quantify the effect the following significance has been computed in [9]:

$$S^{\text{MH}-\delta} \equiv \frac{N^{\text{IH}}(\Delta m_{32}^2 + \delta) - N^{\text{NH}}(\Delta m_{32}^2)}{\sqrt{N^{\text{NH}}(\Delta m_{32}^2)}}, \qquad (42)$$

where δ has been considered as a free parameter. This would correspond to NH as the true hierarchy and Δm_{32}^2 as the true value. The true distribution $N^{\text{NH}}(\Delta m_{32}^2)$ is then fitted by IH distribution with arbitrary values of Δm_{32}^2. It has been found in [9] that the minimum $S_{\text{min}}^{\text{MH}-\delta}$ is reached for $\delta \approx -0.5\sigma(\Delta m_{32}^2)$, where $\sigma(\Delta m_{32}^2)$ is the present 1σ accuracy of determination of Δm_{32}^2 from the global fit [17]. The minimal value (for one year of exposure and no inelasticity information) $S_{\text{min}}^{\text{MH}-\delta} = 3.8$ should be compared with $S^{\text{MH}-\delta}(\delta = 0) = 6.0$, thus showing reduction of the significance by a factor of 1.6.

Future measurements at accelerators will reduce the error by a factor of 2, which means that no significant improvement is expected.

Let us show how information about inelasticity (or use of 3D distributions) may help. As we mentioned before, the effect of a Δm_{32}^2 change is nearly the same for neutrinos and antineutrinos, whereas y distributions are different.

We construct the distribution $S^{\delta,\text{int}}$ and the residual asymmetry plot $S^{\delta,\text{int}} - S^{\text{MH,int}}$ which can be rewritten according to (40) and (41) as

$$S^{\delta,\text{int}} - S^{\text{int}} = -\frac{N^{\text{IH}}(\Delta m_{32}^2) - N^{\text{NH}}(\Delta m_{32}^2 - \delta)}{\sqrt{N^{\text{NH}}(\Delta m_{32}^2)}}.$$

After substitution $(\Delta m_{32}^2 - \delta) \to \Delta m_{32}^2$ this residual asymmetry essentially coincides with the quantity $S^{\text{MH}-\delta}$ (42) computed in [9].

On the left panels of Figs. 8 and 9, we respectively show the plots for the asymmetry S^{int} and for the residual asymmetry $S^{\delta,\text{int}} - S^{\text{int}}$ for an ideal detector after kinematical smearing only. We take $\delta \approx -0.5\sigma(|\Delta m_{32}^2|) = -6 \times 10^{-5}$ eV^2, which corresponds to the maximal degeneracy effect according to [9]. On the right panels of Figs. 8 and 9, we present respectively the asymmetry S^{int} and the residual asymmetry $S^{\delta,\text{int}} - S^{\text{int}}$ after application of the experimental smearing. We used $\sigma_E = \sqrt{0.7E}$, and $\psi_0 = 20°$ as a realistic experimental resolution.
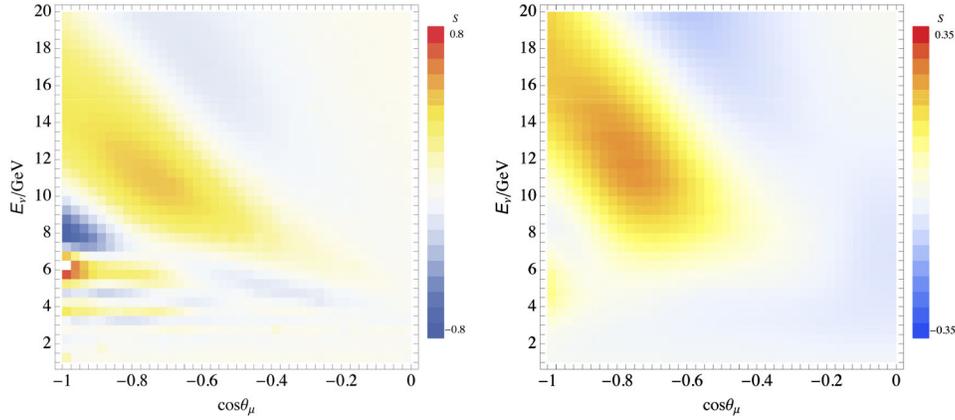
FIG. 8 (color online). Asymmetry plots S^{int} with the kinematical smearing only (left) and after application of the experimental smearing $\sigma_E = \sqrt{0.7E}$, $\sigma_\psi = 20°\sqrt{\frac{m_p}{E_\mu}}$ (right), for one year of exposure.
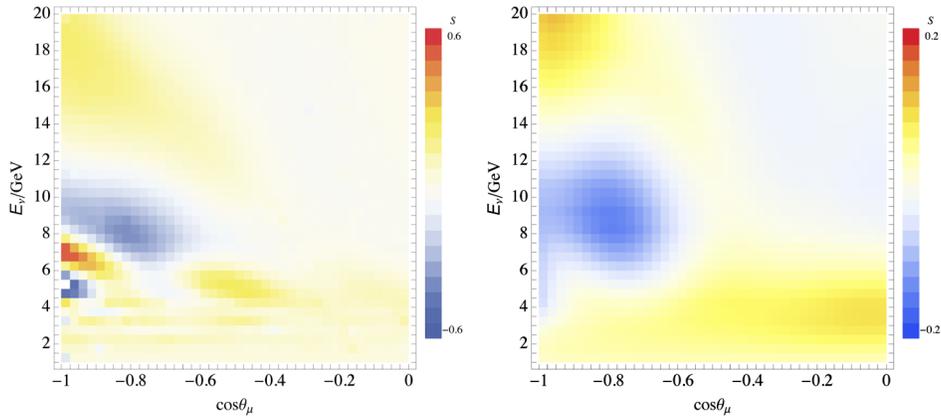

FIG. 9 (color online). Residual asymmetry plots ($S^{\delta,\text{int}} - S^{\text{int}}$) with the kinematical smearing only (left) and after application of the experimental smearing $\sigma_E = \sqrt{0.7E}$, $\sigma_\psi = 20°\sqrt{\frac{m_p}{E_\mu}}$ (right), for one year of exposure.

The total significance of determination of the mass hierarchy can be computed using the residual asymmetry as

$$S_{\text{tot}}^{\text{int}}(\text{MH} - \delta) = \sqrt{\int dE_\nu \int dc_\mu (S^{\delta,\text{int}} - S^{\text{int}})^2}$$

for the distributions without y information, and

$$S_{\text{tot}}(\text{MH} - \delta) = \sqrt{\int dE_\nu \int dc_\mu \int dy (S^\delta - S)^2}$$

with y distribution. For $\delta \approx -0.5\sigma(|\Delta m_{32}^2|)$ and after one year of exposure we obtain $S_{\text{tot}}^{\text{int}}(\text{MH} - \delta) = 4.23$. This should be compared with $S_{\text{tot}}^{\text{int}} = 7.11$ without degeneracy effect (see Table I). So, the degeneracy effect found in such corresponds closely to the one found in [9]. With the y distribution, we obtain $S_{\text{tot}}^{\text{MH}-\delta} = 6.03$ ($S_{\text{tot}} = 8.43$). Thus, the total significance is enhanced by $\sim 43\%$ using the inelasticity.

After the experimental smearing described above we find

$$S_{\text{tot}}^{\text{int}}(\text{MH} - \delta) = 1.93, \qquad S_{\text{tot}}(\text{MH} - \delta) = 2.42$$

(without degeneracy we would have $S_{\text{tot}}^{\text{int}} = 3.87$ and $S_{\text{tot}} = 4.19$, see Table I). The significance enhancement is reduced to about 25%.

These results mean that the necessary exposure to ascertain the mass hierarchy with an ideal detector is a factor of 2 larger if y is not exploited. For the detector with the above-mentioned experimental resolutions, this factor is not as large but it is still significant, about 1.55. The additional relative power of the inelasticity, as we already noticed from the numbers in Table I, is greater, when detector resolutions are better.

VI. DISCUSSION AND CONCLUSIONS

Multimegaton scale under-ice and underwater detectors of atmospheric neutrinos with low (a few GeV) energy thresholds open up new possibilities for the determination

of neutrino properties. This includes the neutrino mass hierarchy, the deviation of the 2–3 mixing from maximal and high accuracy measurement of Δm_{32}^2.

With a dense array of optical modules, it will be possible to identify different atmospheric neutrino events, and in particular, the ν_μ CC events and determine their characteristics. For the ν_μ events, it will be possible to measure not only the energy and the direction of the muon, but also the energy of the accompanying hadron cascade. The latter then determines the inelasticity. With y, one can construct the three-dimensional distributions of events in $(E_\nu, \cos\theta_\mu, y)$.

In this paper, we have explored various improvements of sensitivity to the mass hierarchy, which will be possible with the inclusion of the inelasticity in the analysis. The results can be summarized in the following way.

(1) Inelasticity measurements provide a certain sensitivity to separate signals from neutrinos and antineutrinos. This, in turn, reduces the cancellation of the neutrino and antineutrino contributions to the hierarchy as well as to *CP*-violation effects.

   We find that, in the ideal case of complete separation or independent measurement of ν and $\bar\nu$ signals, the significance of the hierarchy determination increases by a factor of $\sim$2.2–3. However, finite accuracy of the separation (extraction of the parameter α) reduces the effect down to (20–30)%. The best separation is in the range of large y where, however, the angular smearing becomes strong and the effect of mass hierarchy is averaged out.

(2) The selection of events with small y allows one to reduce the angle between the neutrino and muon directions and therefore reduce the kinematical smearing, which is very strong at low energies in the resonance region where the effect of mass hierarchy at the probability level is the biggest one. However, for small y, the effective separation of the ν and $\bar\nu$ contributions worsen, and moreover, the statistics decreases with cut in y. So, for fixed exposure, the overall gain is rather modest.

   Separation of the ν and $\bar\nu$ improves with an increase of y, while the neutrino angle reconstruction improves with a decrease of y. Therefore the analysis of these improvements should be done simultaneously. This requires study of the 3D distributions of events, which takes into account both separation and reduction of kinematical smearing automatically.

(3) We have computed the 3D oscillograms of the ν_μ events with the kinematical smearing (for this the kinematics of the ν_μ CC interactions has been taken into account precisely). We then found the 2D asymmetry distribution in the $E_\nu - \cos\theta_\mu$ plane for different intervals of y. The main contribution to the identification of the hierarchy follows from the intermediate range $y = 0.3$–0.7, and the

contributions from intervals $y = 0.8$–1.0 and $y = 0$–0.2 are small. The inelasticity enhances the total significance of determination of the mass hierarchy by about 20%, which is consistent with our semiqualitative analysis provided that a slight decrease of γ is achieved.

(4) We then performed smearing of the distributions over the observables: the energies of muon and cascade as well as the angle of muon. We used the Gaussian smearing functions assuming different widths and their dependences on energy. The experimental smearing further diminishes the total significance by a factor of 1.5–2.4 depending on the energy and angular resolutions. The inclusion of the inelasticity leads to an increase of the total significance by (8–11)% after application of the experimental smearing: the stronger the smearing, the weaker the significance increase.

(5) Inversion of the mass hierarchy and variations of other parameters have different effects on the y distribution of events. This means that inelasticity measurements will alleviate the degeneracy of the hierarchy with θ_{23} and Δm_{32}^2. Without y distribution the degeneracy with Δm_{32}^2 reduces the significance by a factor of $\sim$1.7. The inelasticity measurements increase the total significance by 43% before the experimental smearing and by 25% with a specific reasonable experimental smearing scheme.

(6) The mass hierarchy and the systematic errors affect the y distribution differently. Therefore measurements of inelasticity will likely help to reduce the impact of systematic uncertainties.

(7) The contamination of the ν_μ event sample with other flavors leads to a suppression of the oscillation effects. The selection of events with not too large y will help discriminate ν_μ CC events from events of other types and therefore mitigate the loss of features in the oscillatory pattern.

(8) All in all, we expect that the inclusion of the inelasticity of the interaction in the analysis will increase the significance by (20–50)%, which is equivalent to an increase of the exposure time or effective volume by a factor of 1.5–2.

(9) It is not excluded that more sophisticated analysis will lead to an even stronger enhancement effect.

The next step in the enhancement of the discovery potential of the multimegaton scale detectors could be related to some information about the direction of the cascade using detailed time information about the development of events. Also the inclusion of other types of events (cascades without muons) in the analysis will reinforce the discovery potential.

The inclusion of the inelasticity as an ingredient in the data analyses may become necessary in order to unambiguously conclude on the mass hierarchy in the near future.

APPENDIX A: VARIABLE CHANGE $\phi \rightarrow c_\nu$

Consider a muon with vector $\boldsymbol{\mu} = (s_\mu, 0, c_\mu)$. The matrix associated to the rotation ϕ around the $\boldsymbol{\mu}$ axis is

$$R_\mu(\phi) = \begin{pmatrix} c_\phi c_\mu^2 + s_\mu^2 & -c_\mu s_\phi & s_{\phi/2}^2 s_{2\mu} \\ c_\mu s_\phi & c_\phi & -s_\phi s_\mu \\ s_{\phi/2}^2 s_{2\mu} & s_\phi s_\mu & c_\mu^2 + c_\phi s_\mu^2 \end{pmatrix}.$$

We consider a neutrino vector $\boldsymbol{\nu}_0$ at an angle β also in the plane x-z. A possible vector is $\boldsymbol{\nu}_0 = (s_{\nu_0}, 0, c_{\nu_0})$, with $\theta_\nu = \theta_\mu + \beta$. We use the matrix to generate revolution vector set $\{\boldsymbol{\nu}(\phi)\}_\phi$ around the muon trajectory,

$$\boldsymbol{\nu}(\phi) = R_\mu(\phi)\boldsymbol{\nu}_0 = \begin{pmatrix} c_\phi c_\mu s_\beta + s_\mu c_\beta \\ s_\phi s_\beta \\ -c_\phi s_\mu s_\beta + c_\mu c_\beta \end{pmatrix}.$$

The z component of the vector $\boldsymbol{\nu}$ can be associated to c_ν,

$$c_\nu = -c_\phi s_\mu s_\beta + c_\mu c_\beta \quad \text{therefore} \quad \mathrm{d}\phi = \mathrm{d}c_\nu/s_\beta s_\mu s_\phi,$$

with $s_\beta s_\mu s_\phi = \sqrt{s_\mu^2 s_\beta^2 - (c_\beta c_\mu - c_\nu)^2}$.

APPENDIX B: SMEARING FUNCTION FOR y

We use the notation $\Delta_\mu \equiv E_\mu - \tilde{E}_\mu$, $\Delta_h \equiv E_h - \tilde{E}_h$, and the simplified relation $y = E_h/(E_\mu + E_h)$. In order to obtain the y distribution, we introduce $z \equiv E_\mu/E_h$, so that $y = 1/(1 + z)$. Consequently, $z = 1/y - 1$ and $\mathrm{d}z = -\mathrm{d}y/y^2$. Let us denote by $P_z(\tilde{z})$ the distribution of $\tilde{z}$. Then the y distribution is given by

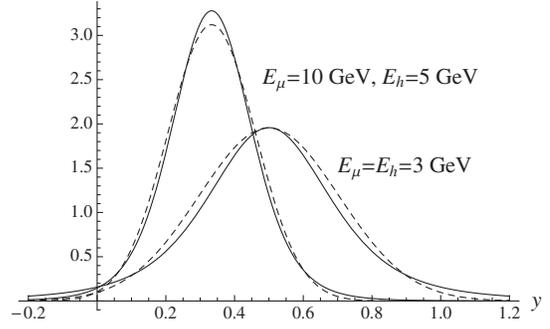$$P_y(\tilde{y}) = \frac{1}{\tilde{y}^2} P_z(1/\tilde{y} - 1).$$

FIG. 10. The reconstructed y distribution for two different sets of $\{E_\mu, E_h\}$ (numbers at the curves) and $\sigma_{\mu,h} = \sqrt{E_{\mu,h}}$. The dashed curves correspond to the Gaussian approximation.

In turn, the distribution of ratio z can be found from

$$P_z(\tilde{z}) = \int g_h(\tilde{E}_h, E_h) g_\mu(\tilde{E}_\mu, E_\mu) \delta\left(\frac{E_\mu}{E_h} - \tilde{z}\right) \mathrm{d}E_h \mathrm{d}E_\mu.$$

The integration gives

$$P_z(\tilde{z}) = \frac{e^{-\frac{\Delta_h^2}{2\sigma_h^2} - \frac{\Delta_\mu^2}{2\sigma_\mu^2}}}{2\pi(\sigma_h^2 + \sigma_\mu^2 \tilde{z}^2)^2 |\Delta_\mu \sigma_h^2 + \Delta_h \sigma_\mu^2 \tilde{z}|}$$
$$\times \left(2\sigma_h \sigma_\mu(\sigma_h^2 + \sigma_\mu^2 \tilde{z}^2)|\Delta_\mu \sigma_h^2 + \Delta_h \sigma_\mu^2 \tilde{z}| \right.$$
$$+ \sqrt{2\pi} e^{\frac{(\Delta_\mu \sigma_h^2 + \Delta_h \sigma_\mu^2 \tilde{z})^2}{2\sigma_h^2 \sigma_\mu^2(\sigma_h^2 + \sigma_\mu^2 \tilde{z}^2)}}(\Delta_\mu \sigma_h^2 + \Delta_h \sigma_\mu^2 \tilde{z})^2$$
$$\left. \times \sqrt{\sigma_h^2 + \sigma_\mu^2 \tilde{z}^2} \mathrm{erf}\left(\frac{|\Delta_\mu \sigma_h^2 + \Delta_h \sigma_\mu^2 \tilde{z}|}{\sqrt{2}\sigma_h \sigma_\mu \sqrt{\sigma_h^2 + \sigma_\mu^2 \tilde{z}^2}}\right) \right).$$

The y distribution obtained in this way is nearly Gaussian in most cases of interest. It starts to deviate from Gaussian, showing enhanced tails, when E_μ and E_h are both small. This is illustrated Fig. 10 for the energy resolution widths $\sigma_{\mu,h} = \sqrt{E_{\mu,h}}$.

[1] E. K. Akhmedov, M. Maltoni, and A. Y. Smirnov, J. High Energy Phys. 05 (2007) 077; 06 (2008) 072; Phys. Rev. Lett. **109**, 091801 (2012).

[2] M. Blennow and A. Yu. Smirnov, Adv. High Energy Phys. **2013**, 972485 (2013).

[3] D. J. Koskinen, Mod. Phys. Lett. A **26**, 2899 (2011).

[4] R. Abbasi et al. (IceCube Collaboration), Astropart. Phys. **35**, 615 (2012).

[5] P. Coyle et al. (KM3NeT Collaboration), in Proceedings of the European Strategy Preparatory Group Symposium, Krakow, Poland, September, 2012 (unpublished).

[6] O. Mena, I. Mocioiu, and S. Razzaque, Phys. Rev. D **78**, 093003 (2008).

[7] E. Fernandez-Martinez, G. Giordano, O. Mena, and I. Mocioiu, Phys. Rev. D **82**, 093011 (2010).

[8] J. Tang and W. Winter, J. High Energy Phys. 02 (2012) 028.

[9] E. K. Akhmedov, S. Razzaque, and A. Y. Smirnov, J. High Energy Phys. 02 (2013) 082.

[10] D. Franco, C. Jollet, A. Kouchner, V. Kulikovskiy, A. Meregaglia, S. Perasso, T. Pradier, A. Tonazzo, and V. Elewyck, J. High Energy Phys. 04 (2013) 008.

[11] S. K. Agarwalla, T. Li, O. Mena, and S. Palomares-Ruiz, arXiv:1212.2238.

[12] M. Ribordy, in *Neutrino Physics and Astrophysics*, edited by G. Bellini and L. Ludhova, Proceedings of ISAPP Course CLXXXII, Varenna, Italy, 2011 (IOS Press, Amsterdam, 2012).

[13] M. Ribordy, Nucl. Instrum. Methods Phys. Res., Sect. A **574**, 137 (2007).

[14] H. L. Lai, J. Huston, S. Kuhlmann, J. Morfin, F. Olness, J. F. Owens, J. Pumplin, and W. K. Tung, Eur. Phys. J. C **12**, 375 (2000).

[15] C. Andreopoulos *et al.*, Nucl. Instrum. Methods Phys. Res., Sect. A **614**, 87 (2010).

[16] M. Salathe, M. Ribordy, and L. Demirors, Astropart. Phys. **35**, 485 (2012).

[17] G. L. Fogli, E. Lisi, A. Marrone, D. Montanino, A. Palazzo, and A. M. Rotunno, Phys. Rev. D **86**, 013012 (2012); M. C. Gonzalez-Garcia, M. Maltoni, J. Salvado, and T. Schwetz, J. High Energy Phys. 12 (2012) 123; D. V. Forero, M. Tortola, and J. W. F. Valle, Phys. Rev. D **86**, 073012 (2012).